PHYSICAL REVIEW D **82,** 114504 (2010)

Update: Precision D_s decay constant from full lattice QCD using very fine lattices

C. T. H. Davies,[1,*] C. McNeile,[1,†] E. Follana,[2] G. P. Lepage,[3] H. Na,[4] and J. Shigemitsu[4]

(HPQCD Collaboration)[‡]

[1]*Department of Physics and Astronomy, University of Glasgow, Glasgow, G12 8QQ, United Kingdom*
[2]*Departamento de Física Teórica, Universidad de Zaragoza, E-50009 Zaragoza, Spain*
[3]*Laboratory of Elementary-Particle Physics, Cornell University, Ithaca, New York 14853, USA*
[4]*Department of Physics, The Ohio State University, Columbus, Ohio, 43210, USA*
(Received 30 August 2010; published 9 December 2010)

We update our previous determination of both the decay constant and the mass of the D_s meson using the highly improved staggered quark formalism. We include additional results at two finer values of the lattice spacing along with improved determinations of the lattice spacing and improved tuning of the charm and strange quark masses. We obtain $m_{D_s} = 1.9691(32)$ GeV, in good agreement with experiment, and $f_{D_s} = 0.2480(25)$ GeV. Our result for f_{D_s} is 1.6σ lower than the most recent experimental average determined from the D_s leptonic decay rate and using V_{cs} from Cabibbo-Kobayashi-Maskawa unitarity. Combining our f_{D_s} with the experimental rate we obtain a direct determination of $V_{cs} = 1.010(22)$, or alternatively $0.990\,^{+0.013}_{-0.016}$ using a probability distribution for statistical errors for this quantity which vanishes above 1. We also include an accurate prediction of the decay constant of the η_c, $f_{\eta_c} = 0.3947(24)$ GeV, as a calibration point for other lattice calculations.

DOI: 10.1103/PhysRevD.82.114504 PACS numbers: 12.38.Gc

I. INTRODUCTION

Lattice QCD is now a firmly established method for providing precision tests of the standard model [1]. Combined with experiment, lattice QCD calculations have the potential to uncover new physics provided that both the theoretical and experimental results are accurate enough.

The most accurate lattice QCD calculations are those for the masses of ''gold-plated'' mesons, where few MeV errors are now possible across the entire spectrum. This accuracy is at the level where electromagnetic effects on the meson masses, currently missing from lattice QCD calculations, have to be estimated and included. Reference [2] gives a recent summary including predictions of masses that have been made ahead of experiment. The meson masses are extracted from simple ''two-point'' hadron correlation functions calculated on the lattice from combining appropriate valence quark and antiquark propagators. Another parallel set of quantities that can be determined from the same correlation functions are the meson decay constants. Calculations of these can be compared to experimental results for rates of annihilation to photons for neutral unflavored vector mesons and to W bosons for charged pseudoscalars. By determining as complete and accurate a picture as possible for decay constants along with masses we provide a stringent test of the standard model. Physics beyond the standard model can introduce new ways to decay to leptons for some mesons, and so accurate comparison of decay constants between theory and experiment can also provide direct constraints on new physics models.

Here we focus on results for one quantity, the decay constant of the D_s meson, f_{D_s}, which has been a showcase for the impact that accurate lattice QCD calculations can have, particularly when ahead of experimental results. We will update our result from 2007 [3], making several improvements to the calculation. It is important to understand that f_{D_s} is not calculated in isolation; as discussed above, it is one piece of the range of QCD physics that is calculable on the lattice. The other pieces, where they can also be tested against experiment, lend weight to the confidence we have in our error analysis. This is particularly true for our calculation because we can calculate a range of different quantities all with the same method. So here we also update our results for the mass of the D_s meson and discuss other calculations that will provide further tests. First we review briefly some background to the calculation of f_{D_s}.

Decay constants for light pseudoscalar mesons (f_π and f_K) have been calculable with errors at the few percent level since 2004 [4], being one of the first calculations done in lattice QCD once ensembles of gluon field configurations were available that included the full effect of u, d and s sea quarks with a light enough mass for the u/d quark to enable controlled extrapolation to the physical point. These calculations were done using the improved staggered (asqtad) formalism [5,6] which has a number of advantages

*c.davies@physics.gla.ac.uk
†Current address: Department of Theoretical Physics, Bergische Universität Wuppertal, Gaussstr. 20, D-42119 Wuppertal, Germany
‡http://www.physics.gla.ac.uk/HPQCD

over previous formalisms, which means that the calculation of f_π and f_K can be done accurately. Key requirements for these calculations are a quark formalism (such as improved staggered quarks) which

(i) has an absolutely normalized operator to couple to the W boson;
(ii) is improved so that it has small discretization errors ($\mathcal{O}(\alpha_s a^2)$ for improved staggered quarks) and
(iii) is numerically fast so that large ensembles of gluon field configurations can be made including sea quarks and so that many hadron correlation functions can be calculated per configuration, for small statistical errors. In addition a large physical volume (> 2.5 fm^3) is necessary so that finite volume effects are reduced to the 1% level. Having all of these features means that accurate extrapolations to the physical continuum limit can be made.

Calculations of decay constants for mesons containing the heavier c quark became important with the promise of results from the CLEO-c experiment. The first lattice results for f_D and f_{D_s} appeared from the Fermilab Lattice/MILC collaborations in 2005 as predictions ahead of experiment [7]. They used the "Fermilab" formalism [8], developed many years previously for heavy quark physics, and had errors of 8%. This led to the unfortunate impression that decay constants for D and D_s mesons were inevitably much less accurate than those for π and K and errors would only be slowly reduced as higher statistics and the advent of finer lattices reduced statistical errors and systematic errors from discretization effects. Because the Fermilab formalism predated the improved staggered formalism, however, these calculations had not made use of any of the features discussed above that made f_π and f_K so accurate.

For c quarks the issue of discretization errors becomes more important than for the lighter quarks. In 2007 we showed that further improving the improved staggered formalism to the highly improved staggered quark (HISQ) formalism [9] produces a quark formalism that has all the good features of the asqtad formalism outlined above but also significantly smaller discretization errors. In fact the discretization errors are small enough that HISQ can be used for c quarks as well as u/d and s quarks and using the same formalism for all 4 lightest quarks has enormous advantages. We used HISQ for all the valence quarks to calculate all 4 decay constants: f_π, f_K, f_D and f_{D_s} to better than 2% accuracy [3]. Our results were

$$\begin{aligned} f_\pi &= 132(2)\ \text{MeV} \qquad f_K = 157(2)\ \text{MeV} \\ f_D &= 207(4)\ \text{MeV} \qquad f_{D_s} = 241(3)\ \text{MeV}. \end{aligned} \tag{1}$$

Although f_D and f_{D_s} still have noticeably larger discretization errors (and therefore contributions to the systematic error from the extrapolation to the $a \to 0$ limit) than f_K and f_π there are smaller systematic errors from, for example, finite volume effects. This leads then to the expectation, and the result, of very similar final errors. Our error for f_{D_s} was somewhat smaller than that for f_D (1.3% versus 1.8%) since the D_s contains no valence u/d quarks and is therefore much less sensitive to the chiral extrapolation to the physical u/d quark mass. This makes f_{D_s} a particularly accurate quantity to calculate in lattice QCD.

Since, at that time, f_D and f_{D_s} were only known to 6–8% from experiment [10–12], we had the added test, unavailable to the Fermilab formalism, of agreeing with experiment for f_π and f_K. An additional very stringent test that had not previously been done was the determination of the mass of the D_s and D mesons along with their decay constants. The masses are known to better than 1 MeV experimentally. We were able to achieve errors from lattice QCD of 7 MeV (0.3%) by determining the difference between the D or D_s mass and one half that of the η_c. Electromagnetic effects on the masses, missing from the lattice QCD calculation, had to be allowed for in achieving this accuracy. Good agreement between lattice QCD and the experimental results was obtained. We quoted $m_{D_s} = 1.962(6)$ GeV and $m_D = 1.868(7)$ GeV [3].

Following our result much improved experimental numbers for f_D [13] (206(9) MeV) and f_{D_s} (274(11) MeV) became available from CLEO [14]. This produced the exciting picture in the summer of 2008 that agreement between experiment and our result for f_D was very good but that the experimental result for f_{D_s} (including averages with results from *BABAR* and Belle [15]) was significantly larger than our lattice QCD value, see, for example, [16,17]. Since the experimental errors were still much bigger than ours the discrepancy, of 3σ, was dominated by the experimental error. A burst of activity from other lattice QCD calculations produced results that agreed with ours but, having errors several times larger, often also agreed with the experimental one [18]. This led to much speculation about the existence of new physics (that had to affect D_s but not D) [19] as well as limits on new physics from the fact that the experimental f_{D_s} was larger (and not smaller) than the standard model result from our calculation [20].

Since then improved statistics and further results from other channels [21–24] have brought down the experimental average and reduced its error to 2%. In early 2010, the Heavy Flavor Averaging Group (HFAG) gave a world average result from experiment of $f_{D_s} = 0.2546(59)$ GeV [25], 2σ above our 2007 result. In the meantime we have extended our lattice QCD calculation using HISQ quarks to even finer lattices as well as improving the accuracy with which we determine the lattice spacing (which provides the calibration of the energy scale) and fix the c and s quark masses. This has led our result for f_{D_s} to move upwards, as we show here, to 0.2480(25) GeV, with a slight improvement in the error to 1%. The main reason for the upward shift is the recalibration of the lattice spacing.

The experimental average as of October 2010 has moved up again slightly with new results from *BABAR* [26]. Our value for f_{D_s} is now 1.6σ from the experimental average and this reduces considerably the room for new physics in this quantity.

In Sec. II we describe the lattice QCD calculation and in Sec. III the results. These sections contain technical details which may not be of interest to those without a lattice QCD background. As well as f_{D_s} we give results for m_{D_s} which, as discussed above, is an important check on the calculation. We also show results for f_{η_c}, the decay constant of the η_c. This cannot be accessed directly from experiment but provides an excellent "figure of merit" for lattice QCD calculations in charm physics. We give the result to 0.6% so that other lattice QCD calculations can compare to this when quoting numbers for f_{D_s}. In Sec. IV we discuss the picture that emerges from the current experimental and lattice QCD results for f_{D_s}, including the update we give here. We have tried to make this section readable by those that skipped the earlier technical details. We will also comment on the effects of the recalibration of the lattice energy scale on the other calculations included in [3], i.e. f_K, f_π and f_D. Section V gives our conclusions.

II. LATTICE QCD CALCULATION

We work with 11 different ensembles of gluon field configurations provided by the MILC Collaboration. These include the effect of u, d and s sea quarks using the improved staggered (asqtad) formalism and the fourth root "trick". This procedure has passed various tests indicating that it is a valid discretization of QCD [27–29]. Configurations are available with large spatial volumes (> 2.4 fm^3) for a wide range of values of the lattice spacing, a, and at multiple values of the sea light and strange quark masses. The u and d quark masses are taken to be equal in the sea ($m_u = m_d = m_l$) for numerical speed. This has negligible effect on the calculations described here. We use configurations at 5 values of the lattice spacing between 0.15 fm and 0.045 fm with parameters as listed in Table I. We have chosen the ensembles so that we can test the dependence of our results on each of: the lattice spacing; the physical volume; the sea light quark mass and the sea strange quark mass.

On these configurations we have calculated quark propagators for charm quarks and strange quarks using the HISQ action. The numerical speed of HISQ means that we have been able to use several nearby quark masses for charm and strange to allow accurate interpolation to the correct values. This is described in the next section. These propagators are combined together to make pseudoscalar meson correlators with valence quark content either "charm-charm," "charm-strange" or "strange-strange." By fitting the correlators as a function of the time separation of the source and the sink on the lattice we are able to determine the ground-state pseudoscalar mass (i.e. that of the η_c, D_s or η_s) and the amplitude with which the ground-state meson is created or destroyed by the local temporal axial current. This latter quantity is directly related to the decay constant.

TABLE I. Ensembles (sets) of MILC configurations with size $L^3 \times T$ and sea mass parameters $m_l^{\rm asq}$ and $m_s^{\rm asq}$ used for this analysis. The sea ASQTAD quark masses ($l = u/d$) are given in the MILC convention where u_0 is the plaquette tadpole parameter. Values of u_0 are given in Table VI. The lattice spacing values in units of r_1 after "smoothing" are given in the second column [31]. Sets 1 and 2 are "very coarse"; sets 3, 4, 5, 6 and 7 "coarse"; sets 8 and 9 "fine"; set 10 "superfine"; and set 11 "ultrafine". The final column gives the number of configurations and the number of time sources per configuration used for calculating quark propagators for the best-tuned parameter sets on each ensemble.

Set	r_1/a	$au_0m_l^{\rm asq}$	$au_0m_s^{\rm asq}$	L/T	$N_{cf} \times N_t$
1	2.152(5)	0.0097	0.0484	16/48	631×2
2	2.138(4)	0.0194	0.0484	16/48	631×2
3	2.647(3)	0.005	0.05	24/64	678×2
4	2.618(3)	0.01	0.05	20/64	595×2
5	2.618(3)	0.01	0.05	28/64	269×4
6	2.644(3)	0.02	0.05	20/64	600×2
7	2.658(3)	0.01	0.03	20/64	328×2
8	3.699(3)	0.0062	0.031	28/96	566×4
9	3.712(4)	0.0124	0.031	28/96	600×4
10	5.296(7)	0.0036	0.018	48/144	201×2
11	7.115(20)	0.0028	0.014	64/192	208×1

The HISQ action [9] is an extension of the asqtad improved staggered quark action, which is itself based on the unimproved (naive) staggered quark action. The unimproved staggered action is equivalent to a simple "naive" discretization of the continuum quark action to give, on the lattice:

$$S = \sum_x \bar{\psi}(x)(\gamma \cdot \Delta(U) + ma)\psi(x), \tag{2}$$

where ma is the quark mass in lattice units. $\Delta(U)$ is a discrete version of the covariant derivative coupling to the lattice gluon field $U_\mu(x)$, which is a set of SU(3) matrices sitting on the links of the lattice:

$$\Delta_\mu(U)\psi(x) = \frac{1}{2}[U_\mu(x)\psi(x+\hat{\mu}) - U_\mu^\dagger(x-\hat{\mu})\psi(x-\hat{\mu})]. \tag{3}$$

In the improved staggered formalism the gluon field in the covariant derivative is smeared i.e. $U_\mu(x)$ is replaced by a sum of products of U_μ matrices tracing out more complicated paths between x and $x + \hat{\mu}$ [5]. The smearing introduces a form factor that reduces the coupling between the quark and high momentum ($p \approx \pi/a$) gluons that cause a particular type of discretization error for staggered quarks. This error in principle appears at $\alpha_s a^2$ but in

practice is very large for unimproved staggered quarks. The error is seen most clearly in the mass differences between different ''tastes'' of pseudoscalar meson, created by different point-split pseudoscalar operators. These mass splittings are proportional to a^2 and are strongly reduced on going from unimproved staggered quarks to improved staggered quarks [6]. Most smearing methods introduce additional discretization errors. This is avoided here by the specific form of the smearing used [5]. In the highly improved staggered quark action this smearing is applied twice with a reunitarization of the gluon field in between. We also apply a projection back on to SU(3) for the gluon field, although this makes little difference in practice. We then find another further large reduction in the splittings between different tastes of pseudoscalar mesons [9]. In the pseudoscalar case the splitting in the squared masses (Δm_π^2) is roughly constant (for quark masses that are not too large) and so the splittings in the pseudoscalar masses themselves (Δm_π) fall with quark mass. Thus these ''taste-changing'' errors are generally smaller for charm quarks than strange quarks [9,32], and they are particularly small with the HISQ action.

Other, more mundane, discretization errors are tackled by standard improvement techniques. A simple analysis in Fourier space of the symmetric difference of Eq. (3) shows that this has errors of $\mathcal{O}(a^2)$ which can be corrected by the addition of a $(pa)^3$ term. This term, known as the Naik term [33], appears in the improved staggered quark action as a mixture of 3-link and 1-link differences. The improved staggered quark action then has discretization errors that are $\mathcal{O}(a^4)$, apart from radiatively generated errors at $\mathcal{O}(\alpha_s a^2)$. The HISQ action uses the same Naik term (except that it contains smeared gluon fields) but corrects it further for discretization errors when using quark masses appropriate to charm or heavier. Discretization errors controlled by the quark mass ma become important in that case. and we adjust the coefficient of the Naik term so that it takes value $(1 + \epsilon)$ instead of 1 [9]. Then, schematically,

$$S = \sum_x \bar{\psi}(x)(\gamma \cdot \tilde{\Delta}(U) + ma)\psi(x), \tag{4}$$

where

$$\tilde{\Delta}_\mu = \Delta_\mu - \frac{1+\epsilon}{6}\Delta_\mu^3. \tag{5}$$

ϵ is a function of ma (starting at $(ma)^2$) calculated to give the correct quark dispersion relation (energy as a function of momentum) at tree level. Here we give an exact formula for ϵ at tree level, $\epsilon_{\rm tree}$, given an expansion for the tree-level pole mass, $m_{\rm tree}$, as a function of the mass ma in the lattice action [9]:

$$m_{\rm tree}a = ma\Big[1 - \frac{3}{80}(ma)^4 + \frac{23}{2240}(ma)^6 + \frac{1783}{537600} \times (ma)^8 - \frac{76943}{23654400}(ma)^{10} + \ldots\Big], \tag{6}$$

$$\epsilon_{\rm tree} + 1 = \frac{4 - \sqrt{4 + \frac{12 m_{\rm tree}a}{\cosh(m_{\rm tree}a)\sinh(m_{\rm tree}a)}}}{(\sinh(m_{\rm tree}a))^2}. \tag{7}$$

These equations are obtained by solving the condition for the ''kinetic mass'', $M_2 = [\partial^2 E/\partial p_x^2]^{-1}$, to be equal to the tree-level pole mass, $m_{\rm tree}$. $m_{\rm tree}$ in turn solves the pole condition at zero momentum. Including a Naik coefficient of $(1 + \epsilon_{\rm tree})$ means that the leading (in the velocity expansion) $(ma)^4$ errors are removed in the HISQ case, and so remaining discretization errors are suppressed either by α_s or by the fact that heavy quarks are nonrelativistic in their bound states. ϵ can be fixed nonperturbatively by demanding that the ''speed of light'' be 1, and this was done in earlier calculations [9]. However it was found that nonperturbative results for ϵ were close to the tree-level result in the HISQ case and so here we simply define ϵ to take the value $\epsilon_{\rm tree}$ above.

It is numerically very fast to calculate quark propagators for staggered actions because they have only one spin component. This means that we can readily calculate propagators from several different time sources on the lattice for improved statistics. Table I lists the number of configurations used from each ensemble and the number of time sources per configuration. To increase statistics further we use a ''random wall'' source for the quark propagator instead of a delta function [4]. The random wall is a set of U(1) random numbers with unit norm on every point of the source time slice (separately for each color) and is used as the source for the inversion to calculate the quark propagator. The same random wall is used for all propagators from a given time source on a given configuration so that when any propagator is combined with the complex conjugate of another to form a meson correlator the random numbers cancel except where the initial spatial points and colors are the same. This effectively increases the number of meson correlators sampled and reduces the statistical noise by a large factor for the case of pseudoscalar mesons. We also take a random starting point for our time sources for the very coarse, coarse and fine ensembles.

The pseudoscalar meson correlation function $C_{ab}(t)$ for meson of valence content $a\bar{b}$ is calculated by multiplying together the quark propagator for quark a and the complex conjugate of the quark propagator for quark b from the same source on a given configuration, matching colors at the source and sink and matching the sink spatial site index, which is summed over to set the meson to zero momentum. The meson correlation function is then averaged over time sources on a single configuration. This means that any correlations between the time sources on a given configuration are accounted for. We also have to worry about autocorrelations between results on successive configurations in an ensemble. Tests by binning correlators have shown that the results on different configurations are independent of each other except on the finest lattices.

We therefore bin the correlators on superfine and ultrafine lattices by a factor of 2.

The correlation function averaged over the independent samples from an ensemble is then fit as a function of the time separation between source and sink, t, to the form:

$$\bar{C}(t) = \sum_i a_i (e^{-M_i t} + e^{-M_i (T-t)}) \tag{8}$$

for the case $a = b$. $i = 0$ is the ground state and larger i values denote radial or other excitations with the same J^{PC} quantum numbers. T is the time extent of the lattice. For the unequal mass case there are additional "oscillating" terms coming from opposite parity states, denoted i_p:

$$\bar{C}(t) = \sum_{i,i_p} a_i e^{-M_i t} + (-1)^t a_{i_p} e^{-M_{i_p} t} + (t \to T - t). \tag{9}$$

To fit we use a number of exponentials i, and where appropriate i_p, in the range 2–6, loosely constraining the higher-order exponentials by the use of Bayesian priors [34]. As the number of exponentials increases, we see the χ^2 value fall below 1 and the results for the fitted values and their errors for the parameters for the ground state $i = 0$ stabilize. This allows us to determine the ground-state parameters a_0 and M_0 as accurately as possible while allowing the full systematic error from the presence of higher excitations in the correlation function. We take the fit parameters to be the logarithm of the ground-state masses M_0 and M_{0_p} and the logarithms of the differences in mass between successive radial excitations (which are then forced to be positive). The Bayesian prior value for M_0 is obtained from a simple "effective mass" in the correlator and the prior width on the value is taken as a factor of 1.5. The prior value for the mass splitting between higher excitations is taken as roughly 600 MeV with a width of a factor of 2. Where oscillating states appear in the fit, the prior value for M_{0_p} is taken as roughly 600 MeV above M_0 with a prior width of a factor of 2 and the splitting between higher oscillating excitations is taken to be the same as for the nonoscillating states. The amplitudes a_i and a_{i_p} are given prior widths of 1.0.

Our fit includes the effect of correlation between different values of t. We apply a cut on the range of eigenvalues from the correlation matrix that are used in the fit of 10^{-3} or 10^{-4}. We also cut out very small t values from our fit, typically below 3 or 4, to reduce the effect of higher excitations.

The results for masses and amplitudes from fits in Eqs. (8) and (9) are in units of the lattice spacing. The value of the lattice spacing must be determined for each ensemble to enable conversion to physical units. For this we use the parameter r_1, defined from the heavy quark potential [4]. This parameter can be accurately determined (to better than 0.5%) in units of the lattice spacing and so is good for making ensemble to ensemble comparisons of a. Results from the MILC Collaboration are given in Table I.

Unfortunately r_1 does not have a directly accessible physical value. Instead we must determine that from other quantities. In [35] we used four other physical quantities with well-known experimental values to fix the value of r_1 to 0.3133(23) fm. This then yields a value for a on a given ensemble with two errors—an error from the value of r_1/a on that ensemble and an error, correlated between ensembles, from the physical value of r_1.

The amplitude, a_0, from the fits in Eqs. (8) and (9) is directly related to the matrix element for the local pseudoscalar operator to create or destroy the ground-state pseudoscalar meson from the vacuum. From the definition of the correlator and using a relativistic normalization for the fields:

$$a_0 = (\langle 0|P_s|P\rangle)^2/2M_0 \tag{10}$$

where the pseudoscalar current $P_s = \bar{a}\gamma_5 b$ for quark content $a\bar{b}$. Because of the chiral symmetry of the staggered quark action we have a partially conserved axial current (PCAC) relation that relates the local pseudoscalar operator above to a temporal axial current that is absolutely normalized on the lattice. This allows us to determine the decay constant for these pseudoscalar mesons without having to worry about an uncertainty from the renormalization between the lattice and the continuum. The decay constant for meson P with quark content $a\bar{b}$ is defined from

$$\langle 0|\bar{a}\gamma_\mu\gamma_5 b|P(p)\rangle \equiv f_P p_\mu. \tag{11}$$

For a meson at zero momentum, and using the PCAC relation $\partial_\mu A^\mu = (m_a + m_b)P_s$ to relate the axial vector and pseudoscalar currents, this becomes

$$(m_a + m_b)\langle 0|\bar{a}\gamma_5 b|P(p)\rangle \equiv f_P M_P^2, \tag{12}$$

where m_a and m_b are the appropriate quark masses. Combining this with Eq. (10) then allows us to determine f_P in lattice QCD from our fits to the correlators for pseudoscalar meson P using

$$f_P = (m_a + m_b)\sqrt{\frac{2a_0}{M_0^3}}. \tag{13}$$

Here m_a and m_b are the quark masses used in the lattice QCD calculation.

f_P in turn is related, for charged pseudoscalars such as the π, K, D and D_s mesons, to the experimentally measurable leptonic branching fraction via a W boson:

$$\mathcal{B}(P \to l\nu_l(\gamma)) = \frac{G_F^2 |V_{ab}|^2 \tau_P}{8\pi} f_P^2 m_l^2 m_P \left(1 - \frac{m_l^2}{m_P^2}\right)^2, \tag{14}$$

up to calculable electromagnetic corrections. V_{ab} is the appropriate Cabibbo-Kobayashi-Maskawa (CKM) element for quark content $a\bar{b}$. τ_P is the pseudoscalar meson lifetime.

III. RESULTS

Accurate results for the D_s meson require accurate tuning of both the c and the s quark masses. We use the pseudoscalar mesons made purely of c quarks or of s quarks to do this and so first discuss results for these mesons.

Table II lists the valence HISQ quark masses close to that of the charm quark that we used for each of the gluon configuration ensembles along with the corresponding value of the Naik parameter $(1 + \epsilon)$. We also list the values of the ground-state pseudoscalar $c\bar{c}$ meson mass and decay constant obtained from our fits to the $c\bar{c}$ meson correlators to Eq. (8). The decay constant, f_{η_c}, will be discussed in Sec. III C—it is a useful quantity to calculate despite the fact that the η_c is a neutral particle and does not undergo a purely leptonic decay of the kind given in Eq. (14). To tune the charm quark mass in the HISQ action we must interpolate to the point at which the mass of the η_c has the correct physical value on each ensemble. This physical value is not exactly the experimental value (2.980 GeV [37]) because our lattice QCD calculation corresponds to a world in which there are no electromagnetic interactions and we do not allow our η_c meson to annihilate to gluons. Both of these effects tend to reduce the η_c mass by small amounts and so the appropriate physical value for us to compare our lattice QCD calculation to is 2.985(3) GeV, allowing a 50% error for each correction to the experimental value. The corrections are obtained from a potential model for the electromagnetic effect and from perturbation theory for the effect of gluon annihilation [9,35].

Figure 1 shows the meson mass in physical units plotted against the quark mass, also in physical units, for each ensemble. This plot demonstrates how the quark mass tuning is done, as well as illustrating very clearly how accurately we can do this from lattice QCD. Several features of the figure stand out. On a given ensemble the value of the meson mass is linear in the quark mass, as we would

TABLE II. Results for the masses in lattice units of the goldstone pseudoscalars made from valence HISQ charm or strange quarks on the different MILC ensembles, enumerated in Table I. Columns 2 and 3 give the corresponding bare charm quark mass, and Naik coefficient, respectively. Column 6 gives the bare strange quark mass ($\epsilon = 0$ in that case). A lot of the meson masses in this table appear also in [36] but we have added results on the coarse 02/05 and 01/03 ensembles (sets 6 and 7) and the large volume coarse 01/05 ensemble (set 5) as well as improving the tuning of masses on other ensembles and improving some fits on sets 4, 10 and 11. Results for the decay constant of the η_c meson are also included, for analysis in Sec. III C.

Set	am_c	$1+\epsilon$	am_{η_c}	af_{η_c}	am_s	am_{η_s}
1	0.81	0.665	2.19381(16)	0.3491(5)	0.061	0.50490(36)
	0.825	0.656	2.22013(15)	0.3539(5)	0.066	0.52524(36)
	0.85	0.641	2.26352(15)	0.3622(5)	0.080	0.57828(34)
2	0.825	0.656	2.21954(13)	0.3537(4)	0.066	0.52458(35)
3	0.622	0.779	1.79132(8)	0.25706(18)	0.0489	0.41133(17)
	0.65	0.762	1.84578(8)	0.26368(18)	0.0537	0.43118(18)
4	0.63	0.774	1.80849(11)	0.25998(20)	0.0492	0.41436(23)
	0.66	0.756	1.86666(10)	0.26721(20)	0.0546	0.43654(24)
	0.72	0.720	1.98109(10)	0.28228(22)	0.06	0.45787(23)
	0.753	0.700	2.04293(10)	0.29114(24)	0.063	0.46937(24)
5	0.63	0.774	1.80856(7)	0.26006(15)	0.0492	0.41457(14)
6	0.625	0.777	1.79347(13)	0.2556(3)	0.0491	0.41196(24)
					0.0525	0.42588(30)
					0.0556	0.43834(30)
7	0.619	0.781	1.78595(15)	0.2564(3)	0.0487	0.41030(31)
8	0.413	0.893	1.28057(7)	0.17217(11)	0.0337	0.29413(12)
	0.43	0.885	1.31691(7)	0.17508(11)	0.0358	0.30332(12)
	0.44	0.880	1.33816(7)	0.17678(11)	0.0366	0.30675(12)
	0.45	0.875	1.35934(7)	0.17850(11)	0.0382	0.31362(14)
9	0.412	0.894	1.27522(7)	0.17086(10)	0.0336	0.29309(13)
	0.427	0.885	1.30731(10)	0.17344(15)	0.03635	0.30513(20)
10	0.273	0.951	0.89935(12)	0.11864(24)	0.0228	0.20621(19)
	0.28	0.949	0.91543(8)	0.11986(21)	0.024	0.21196(13)
11	0.193	0.975	0.66628(13)	0.0882(3)	0.0161	0.15278(28)
	0.195	0.975	0.67117(6)	0.08846(11)	0.0165	0.15484(14)
					0.018	0.16209(17)

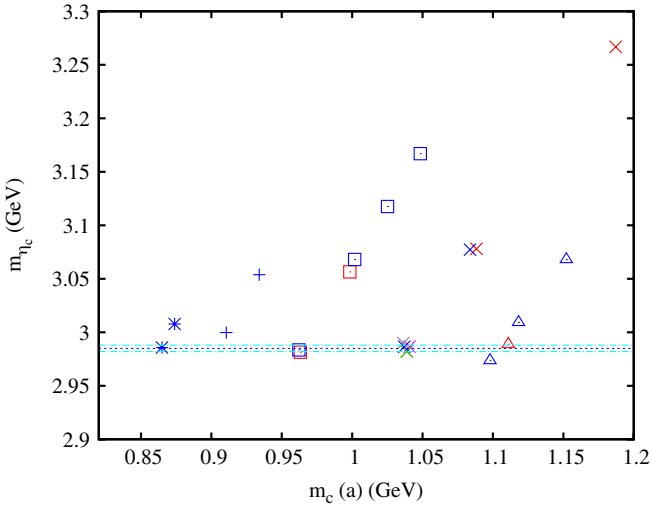

FIG. 1 (color online). Results for the mass of the pseudoscalar meson made of quarks with masses close to that of the charm quark mass for the full set of ensembles from Table I. The x-axis is the lattice bare mass of the quark, which runs with lattice spacing from right to left. Very coarse ensembles are triangles; coarse, crosses; fine, squares; superfine, pluses; ultrafine, bursts. Results for heavier sea u/d quark masses at each lattice spacing are in red, lighter ones are in blue. On the coarse lattices the very heavy sea masses of set 6 are in pink, the lighter strange sea mass of set 7 in grey and the large volume results on set 5 are in green, on top of the result from set 4. Statistical errors are too small to be visible on this plot. The results show that tuning the quark mass to that of charm depends very little on the sea-quark masses or on the volume. The dotted line gives the physical value, with its error, appropriate to lattice QCD, see text.

expect. The lines showing this behavior (not plotted on the figure) are essentially parallel with a slope close to the naive expectation of 2 for ensembles with different lattice spacing values. In fact the slope does increase from 1.7 on the very coarse lattices to 2.3 on the superfine lattices. The reason for this is that the x-axis is a well-defined "running" quark mass, being the quark mass in the HISQ Lagrangian with a particular ultraviolet scale set by the lattice spacing. This is why we denote the mass on the x-axis as $m_c(a)$. The horizontal line indicates the correct value of the η_c mass and therefore, where it cuts each set of results, the tuned value of m_c at that lattice spacing. These values "run" to the left on finer lattices as the ultraviolet cutoff increases, as expected from perturbation theory. We expect the variation of η_c mass with quark mass to be some number (say, 2) times the quark mass at a fixed scale. Therefore on finer lattices, where the scale is higher, we expect the slope to be larger, as demonstrated in Fig. 1.

Another feature is that the results for different ensembles with very similar values of the lattice spacing are very close together i.e. there is very little dependence of the tuned c mass on the sea-quark masses. The results for different physical volumes (sets 4 and 5) lie on top of each other showing that there is no dependence on the volume. We would not expect any significant volume dependence on these large spatial volumes for the η_c since it is a relatively small particle.

From the horizontal line on Fig. 1 and the lattice points on the line it is clear that we have tuned the charm quark mass very well on all except the superfine lattices (where it is off by 0.1%). In each case this corresponds to the lightest charm quark mass in our Table II. Figure 1 does not include errors in converting the lattice quark mass or η_c mass to GeV coming from the values of r_1/a or the physical value of r_1. The effect of these errors is reduced over naive expectations because Δm_{η_c} is close to $2\Delta m_c$, and so the leading-order change from any Δa cancels out. This issue was addressed in [36]. Here we are not aiming to determine m_c, but simply to make sure we understand the errors in other quantities induced by the tuning error in $m_c a$, so we leave a more detailed discussion of this source of systematic error to the sections on the individual quantities.

Table II lists the valence HISQ quark masses close to that of the strange quark that we used for making strange quark propagators on each of the gluon field ensembles. We also list the corresponding values of the mass of the ground-state $s\bar{s}$ meson, the η_s. The η_s is not a particle available to study in the real world where $s\bar{s}$ mixes with $u\bar{u}$ and $d\bar{d}$. However, by omitting these possibilities in the lattice QCD calculation we can obtain a pure $s\bar{s}$ "pion-like" meson. This turns out to be useful for tuning the s quark mass because the η_s mass can be determined relatively precisely, and is less sensitive to the sea-quark masses than, for example, m_π. However, the physical value for the η_s mass has to be determined by relating it to π and K meson masses known from experiment. In earlier lattice QCD calculations we determined $m_{\eta_s} = 0.6858(40)$ GeV [35] and this is the value we will use here. We also studied the η_s decay constant which is again a quantity that cannot be measured experimentally in the real world but one which turns out to be useful for determining the lattice spacing. We will not discuss f_{η_s} further here.

Figure 2 shows the square of the η_s mass against the quark mass, both in physical units, for each ensemble. We expect $m^2_{\eta_s} \propto m_s$ from leading-order chiral perturbation theory and the results indeed show this dependence. Once again the lines demonstrating this (not plotted on the figure) are fairly parallel but with a slope increasing on the finer lattices as the quark mass for a given meson mass runs to smaller values. The horizontal plots gives the physical value of the η_s mass given above and the strange quark mass can be read off for each ensemble from where this crosses the line of data. Again we have well-tuned strange quark masses at each value of the lattice spacing at the lightest end of the range. The strange quark mass values on the very coarse and coarse lattices are rather close together but on the finer lattices the strange mass changes as rapidly with lattice spacing as the charm mass does in

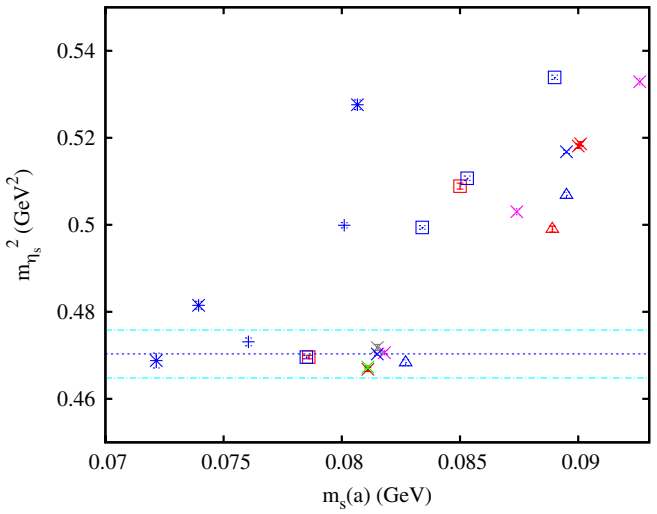

FIG. 2 (color online). Results for the square of the mass of the pseudoscalar meson made of quarks with masses close to that of the strange quark mass for the full set of ensembles from Table I. Errors are statistical errors from the fits to the meson correlators. The x-axis is the lattice bare mass of the quark, which runs with lattice spacing from right to left. Very coarse ensembles are triangles; coarse, crosses; fine, squares; superfine, pluses; ultrafine, bursts. Results for heavier sea u/d quark masses at each lattice spacing are in red, lighter ones are in blue. On the coarse lattices the very heavy sea masses of set 6 are in pink, the lighter strange sea mass of set 7 in grey and the large volume results on set 5 are in green, on top of the result from set 4. The results show that tuning the quark mass to that of strange depends very little on the sea-quark masses or on the volume. The dotted line gives the physical value, with its error, appropriate to lattice QCD, see text.

Fig. 1. In the continuum limit the ratio of these two masses becomes a scale-invariant constant [36].

Again it is evident from Fig. 2 that there is very little dependence of the tuned s quark mass on either the sea-quark masses or the volume. Because the value of the tuned s quark mass is proportional to the square of the η_s mass the relative uncertainty in m_s arising from lattice spacing errors is equal to that of the lattice spacing. There is no cancellation as there was in the case of the charm quark. In addition the 0.6% uncertainty in the physical value of the η_s mass is significant, because it becomes an uncertainty of 1.2% in m_s. The effect of these uncertainties on the mass and decay constant of the D_s meson will be discussed below.

The staggered quarks in the sea are asqtad improved staggered quarks rather than HISQ quarks, i.e. they use a different discretization of the quark piece of the QCD Lagrangian. The s quark mass in the two formalisms will then not be the same, and we need to understand the ratio of the two so that we can extrapolate to the physical (real world) point for both the valence and sea-quark masses. We can determine the physical points for the sea-quark masses from our tuning of the valence masses and this ratio. There is very little sea-quark mass dependence in the quantities that we study here, so that we do not need to know this ratio accurately. It is discussed further in the Appendix.

Once we have determined the c and s masses to be used to give the required physical results for the η_c and the η_s mesons, the D_s meson correlator is entirely prescribed. There are no further adjustable parameters, given the nature of QCD. The fit to the D_s meson correlators gives us both the D_s meson mass (from M_0 in Eq. (9)) and its decay constant (from a_0) as testable outputs from lattice QCD. Since the D_s meson mass is well-known experimentally it provides an excellent independent test of the error analysis on the decay constant. It is therefore very important to analyze both of these quantities together.

A. m_{D_s}

The D_s meson correlators are made from the same c and s quark propagators that are used for the η_c and η_s above. We must use Eq. (9) to fit the D_s correlators, however, because they do have additional oscillating terms in them. Table III lists results for the masses, M_0 and the decay constant derived from a_0 for each combination of c and s masses that we have used on each ensemble. The statistical errors coming from the fit are significantly larger for the D_s than for the η_c. This is because the noise in heavy-light correlators has a lower mass associated with it than the signal. The mass in the squared correlator which gives the noise is given by one half of the sum of the η_c and η_s masses, which is smaller than the signal D_s mass. This means that the signal to noise ratio degrades at large times for the D_s correlator and the statistical error increases. This is illustrated in Fig. 3 in which we explicitly plot and compare the ''effective mass'' extracted from the D_s correlator and from its statistical error. This issue becomes a problem for B meson correlators [38]. It is not a big problem for the D_s, however, and the statistical errors that we obtain in Table III are very small.

To determine the physical mass of the D_s meson as accurately as possible we want to minimize errors coming from the conversion from lattice units to physical units i.e. from the lattice spacing. The error on the physical value of r_1 is 0.7%. Applied directly to the D_s mass this would amount to a sizeable 14 MeV error. This can be avoided however, by calculating instead the mass difference $m_{D_s} - m_{\eta_c}/2$. Because this is much smaller (480 MeV) it will have a much reduced absolute error from the lattice spacing [3]. In addition, it is much less sensitive to any errors from mistuning of the c quark mass because the leading contribution of m_c effectively cancels in this difference. Indeed this difference can be thought of as the difference in binding energy between a charmonium meson and a charm-light meson, and is therefore an important physical quantity. The fact that it can be calculated accurately in lattice QCD and compared to experiment is a stringent test of QCD itself.

TABLE III. Results for the mass and decay constant of the D_s meson in units of the lattice spacing for a range of charm and strange quark masses on each MILC ensemble.

Set	am_c	am_s	am_{D_s}	af_{D_s}
1	0.81	0.061	1.4665(8)	0.1970(10)
	0.825	0.066	1.4869(7)	0.1994(10)
	0.825	0.080	1.5019(6)	0.2042(8)
	0.85	0.066	1.5117(8)	0.2004(10)
	0.85	0.080	1.5266(6)	0.2053(9)
2	0.825	0.066	1.4869(11)	0.1997(20)
3	0.622	0.0489	1.1890(7)	0.1538(9)
	0.65	0.0537	1.2247(5)	0.1561(9)
4	0.63	0.0492	1.2007(5)	0.1559(7)
	0.66	0.0546	1.2391(5)	0.1586(6)
	0.66	0.06	1.2452(5)	0.1604(6)
	0.66	0.063	1.2486(4)	0.1614(6)
	0.72	0.0546	1.3027(6)	0.1602(7)
	0.72	0.06	1.3086(5)	0.1620(7)
	0.72	0.063	1.3120(5)	0.1631(6)
	0.753	0.0546	1.3369(6)	0.1610(7)
	0.753	0.06	1.3429(5)	0.1629(7)
	0.753	0.063	1.3462(5)	0.1639(7)
5	0.63	0.0492	1.2013(5)	0.1561(8)
6	0.625	0.0491	1.1916(7)	0.1553(10)
7	0.619	0.0487	1.1867(10)	0.1548(17)
8	0.413	0.0337	0.84721(23)	0.10836(24)
	0.43	0.0358	0.86982(23)	0.10943(24)
	0.43	0.0366	0.87079(22)	0.10970(24)
	0.43	0.0382	0.87274(21)	0.11028(24)
	0.44	0.0358	0.88152(23)	0.10959(27)
	0.44	0.0366	0.88249(23)	0.10986(27)
	0.44	0.0382	0.88443(22)	0.11044(24)
	0.45	0.0358	0.89317(24)	0.10974(27)
	0.45	0.0366	0.89414(23)	0.11001(27)
	0.45	0.0382	0.89607(23)	0.11059(27)
9	0.412	0.0336	0.84352(26)	0.10779(31)
	0.427	0.03635	0.86443(40)	0.1086(5)
10	0.273	0.0228	0.59350(24)	0.07500(27)
11	0.193	0.0161	0.43942(33)	0.05533(39)
	0.195	0.0165	0.44270(28)	0.05550(34)

The first stage in the analysis of the D_s meson mass is to determine the difference $m_{D_s} - m_{\eta_c}/2$ for tuned c and s quark masses on each ensemble. As discussed above, we have results very close to the tuned point on almost every one of the 11 ensembles. However, it is important to make sure that all of our results are tuned to the same point before extrapolation and so we first test the dependence of $m_{D_s} - m_{\eta_c}/2$ as a function of m_s and m_c. Figs. 4 and 5 show results as a function of $m^2_{\eta_s}$ and m_{η_c} for sets 1, 4 and 7 where we have multiple data points with different combinations of m_c and m_s and so can unravel the separate dependences. The dependence is plotted against meson mass rather than directly against the quark mass since the tuning condition is set by the η_c or η_s meson mass, so this is a more direct (and more physical) way to study any mistuning effects. Note that the mass values of the η_c and η_s are above their physical values for the cases given in Figs. 4 and 5. Since we are only studying small mistuning effects for the values of the masses that we have closer to

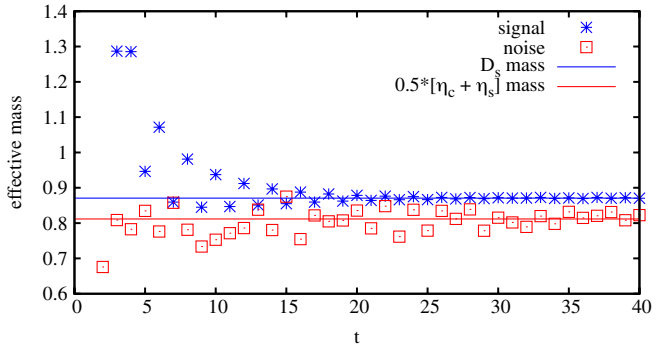

FIG. 3 (color online). Results for the effective mass of the D_s correlator and the effective mass of the noise in the D_s correlator plotted as a function of lattice time for one correlator on the fine lattices (set 8). The effective mass is obtained from the log of the ratio of the correlator (or its error) at successive times. At large times it becomes the mass of the lowest state in the correlator or its error. The lines compare the results to the expected mass i.e. the D_s mass for the signal and $(m_{\eta_s} + m_{\eta_c})/2$ for the noise.

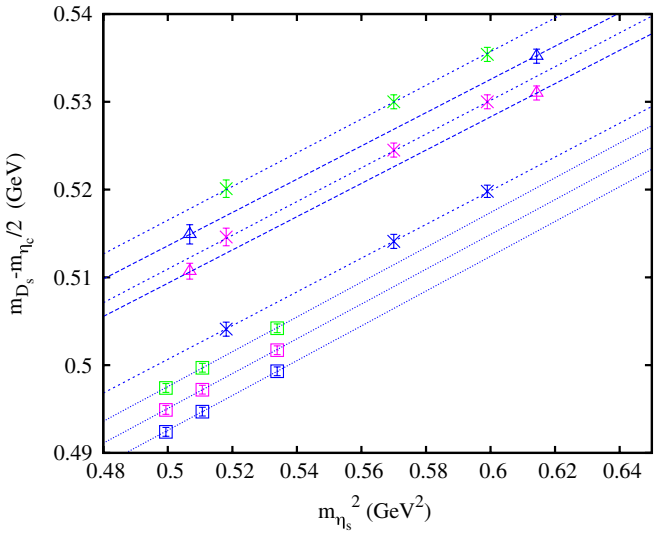

FIG. 4 (color online). Results for the mass of the D_s meson (specifically the difference between that mass and one half of the η_c mass) as a function of the square of the η_s meson mass, acting as a proxy for the strange quark mass. Results are for a range of different quark masses around the masses of the c and s quark masses on very coarse set 1 (triangles), coarse set 4 (crosses) and fine set 7 (squares). The lines are fits to the results for each ensemble allowing linear terms in $m^2_{\eta_s}$ and m_{η_c}. Here the lines join points for a fixed c quark mass. See Fig. 5 for the equivalent as a function of m_{η_c}.

the physical points, this will give a sufficiently accurate picture of these effects.

In Fig. 4 we see that the dependence of $m_{D_s} - m_{\eta_c}/2$ on $m^2_{\eta_s}$ is linear as we expect, since this corresponds to a linear dependence on m_s. The slope is clearly physical i.e. independent of the lattice spacing (whereas the slope against m_s would not be, because of the running of m_s itself, discussed earlier). The value of the slope is 0.20(1) and this can be compared to an "experimental" slope, albeit over a much larger mass range, of 0.22 obtained by comparing results for the masses of the D and the D_s [37]. Figure 5 also shows linear dependence on m_c, expressed physically as linear dependence on m_{η_c}. The slope does differ on the very coarse lattices from the others so showing some lattice spacing dependence in this case. The slope is also very small $\sim$0.05 because, as discussed above, the leading dependence on m_c cancels between m_{D_s} and $m_{\eta_c}/2$. The slope is again similar to the "experimental" value of 0.03 obtained over a much larger mass range from comparing B_s and D_s mesons [37].

Results from Figs. 4 and 5 can be used to adjust the values of $m_{D_s} - m_{\eta_c}/2$ on each ensemble to the tuned point, $m_{\eta_c} = 2.985$ GeV and $m_{\eta_s} = 0.6858$ GeV. An error of 50% of any shift is added in quadrature to the statistical error. The shifts from mistuning are less than the statistical error on all ensembles except sets 2 (very coarse) and 10 (superfine). On set 10 the shift is by 1.5 times the statistical error and on set 2 by 4 times the statistical error. Table IV gives the tuned value of $m_{D_s} - m_{\eta_c}/2$ in GeV on each ensemble along with two errors. The first is the statistical/tuning error and the second is that from the error in r_1/a on that ensemble. This error is a factor of 3 smaller than its naive value because of a cancellation of lattice spacing errors inside the mass difference. Any change in r_1/a means a change to m_{η_c} and m_{η_s} as well as a change in $m_{D_s} - m_{\eta_c}/2$. The results then need to be retuned to the physical c and s masses and this largely cancels the change resulting from the change in r_1/a. The error from r_1/a uncertainty is much smaller than the statistical error then in every case. The statistical errors, which dominate, are at the level of 1 MeV.

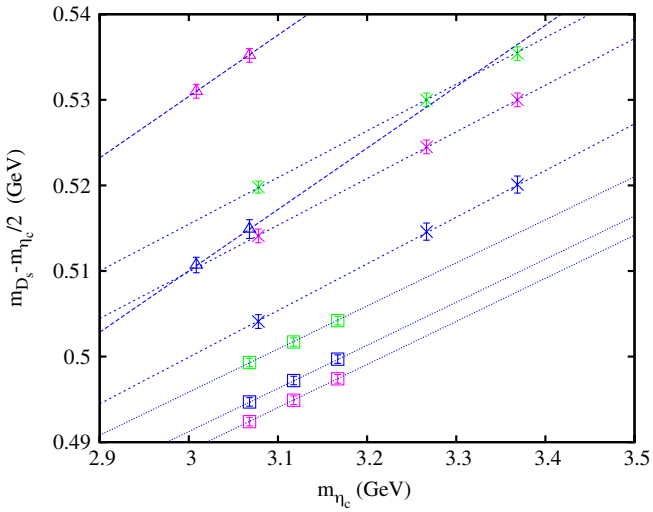

FIG. 5 (color online). Results for the mass of the D_s meson (specifically the difference between that mass and one half of the η_c mass) as a function of the η_c meson mass, acting as a proxy for the charm quark mass. Results are for a range of different quark masses around the masses of the c and s quark masses on very coarse set 1 (triangles), coarse set 4 (crosses) and fine set 7 (squares). The lines are fits to the results for each ensemble allowing linear terms in $m^2_{\eta_s}$ and m_{η_c}. Here the lines join points for a fixed s quark mass. See Fig. 4 for the equivalent as a function of $m^2_{\eta_s}$.

We can then extrapolate the tuned values on each ensemble in the lattice spacing and the sea-quark masses to the physical point where the lattice spacing is zero and the sea-quark masses take their real world values. It is clear from Table IV looking at the coarse and fine ensembles that $m_{D_s} - m_{\eta_c}/2$ has no significant dependence on the sea-quark masses at the level of our 1 MeV statistical errors. The picture is obscured on the very coarse lattices by the larger error on set 2 from mistuning. In fact if we compare sets 1 and 2 at the η_c and η_s masses corresponding to those available on set 2 (i.e. at somewhat heavier masses than the correctly tuned point) then we find again that sets 1 and 2 agree on the value of $m_{D_s} - m_{\eta_c}$ but now within an error of 1.5 MeV rather than the 3 MeV in Table IV.

We expect $m_{D_s} - m_{\eta_c}/2$ to be very insensitive to the sea-quark masses based on chiral perturbation theory. This couples a nonrelativistic Lagrangian for D and D_s meson fields to the pion octet and gives an expansion in powers of π, K and η_8 masses for the mass and decay constant of the appropriate D meson. The D_s has valence c and s masses

TABLE IV. Values for the mass and decay constant of the D_s meson and for the decay constant of the η_c after tuning to the physical c and s masses (i.e. the physical η_c and η_s meson masses) on each ensemble. Results are in GeV with two errors, the first from statistics and tuning and the second from the uncertainty in r_1/a on that ensemble.

Set	$m_{D_s} - \frac{m_{\eta_c}}{2}$ (GeV)	f_{D_s} (GeV)	f_{η_c} (GeV)
1	0.5021(12)(4)	0.2674(14)(3)	0.4753(9)(2)
2	0.5020(32)(4)	0.2671(28)(3)	0.4756(6)(2)
3	0.4889(12)(3)	0.2564(15)(2)	0.4284(3)(1)
4	0.4897(9)(3)	0.2573(12)(2)	0.4291(4)(1)
5	0.4906(9)(3)	0.2576(13)(2)	0.4292(4)(1)
6	0.4909(12)(3)	0.2586(17)(2)	0.4255(5)(1)
7	0.4911(17)(3)	0.2592(28)(2)	0.4286(6)(1)
8	0.4823(6)(2)	0.2525(6)(2)	0.4012(3)(2)
9	0.4817(6)(2)	0.2520(7)(2)	0.3998(3)(2)
10	0.4784(10)(2)	0.2499(9)(3)	0.3945(10)(3)
11	0.4766(13)(4)	0.2481(17)(5)	0.3953(13)(6)

which have been tuned to the appropriate values so the only dependence we are interested in here is the dependence on sea s and u/d quark masses which enter through the masses of mesons made either purely of sea quarks or of mixed sea and valence quarks. The leading tree-level dependence on sea-quark masses is a term $C(2m_{l,\mathrm{sea}} + m_{s,\mathrm{sea}})$. Loops couple the D_s meson to a virtual DK or $D_s\eta_8$ pair. This generates logarithmic terms but with, in this case, a very benign dependence on sea-quark masses since none of the associated meson masses vanish in the chiral limit. These terms can then simply be viewed as additional polynomial terms in $m_{l,\mathrm{sea}}$ and $m_{s,\mathrm{sea}}$. A more detailed chiral analysis is not useful here because the sea-quark mass dependence of our results is clearly so small as to have no useful information in it. We simply need to make sure that we allow a sufficient error on the extrapolated value at the physical point to allow for any sea-quark mass dependence that might be there. For this purpose a simple polynomial expansion in $m_{l,\mathrm{sea}}$ and $m_{s,\mathrm{sea}}$ suffices. We take as expansion coefficients δx_l and δx_s where $\delta x_q = (m_{q,\mathrm{sea}} - m_{q,\mathrm{sea,phys}})/m_{s,\mathrm{sea,phys}}$. $m_{s,\mathrm{sea,phys}}$ is the sea (asqtad) strange quark mass at the physical point. We take this value from results quoted by the MILC Collaboration [31] for very coarse to superfine and use the analysis of the ratio of HISQ to asqtad mases from the Appendix to give the value of $m_{s,\mathrm{sea,phys}}$ on the ultrafine lattices. We take $m_{l,\mathrm{sea,phys}} = m_{s,\mathrm{sea,phys}}/27.2$ using the ratio for m_l/m_s determined by the MILC Collaboration [31]. Table IV shows that $m_{D_s} - m_{\eta_c}/2$ does have significant dependence on the lattice spacing, changing by 20 times the statistical error between very coarse and ultrafine lattices. This is also not surprising because the charm quark is relatively heavy and consequently the scale for discretization errors here will be much higher than that for quantities involving only light quarks. This is why it is important to have a formalism, such as HISQ, with very well controlled discretization errors and to have results at many values of the lattice spacing. Discretization errors with the HISQ action can appear only as powers of a^2—no odd powers of a are allowed. The a^2 errors appearing at tree-level have been removed and so the coefficient of a^2 terms is $\mathcal{O}(\alpha_s)$. The inclusion of the Naik term with coefficient calculated at tree-level means that all $(m_c a)^{2n}$ discretization errors are removed at leading order in v^2/c^2 where v^2 is the velocity of the charm quark in the D_s or η_c. Thus discretization errors from the HISQ action are expected to be at the level of $(v^2/c^2)(m_c a)^{2n}$, except for the a^2 term which is further suppressed by α_s. There are additional $\alpha_s a^2$ and tree-level a^4 and higher errors coming from the gluon action, however. These we would typically expect to have a scale of a few hundred MeV (i.e. Λ_{QCD}) associated with them rather than m_c, so their effects will be included if we allow for a scale of m_c.

We therefore take the following fit form to extrapolate $\Delta = m_{D_s} - m_{\eta_c}/2$ to the physical point:

$$\begin{aligned}\Delta(a, \delta x_l, \delta x_s) &= \Delta_{\mathrm{phys}}\Big[1 + \sum_{j=1}^{4} c_j (m_c a)^{2j} + 2b_l \delta x_l (1 + c_b (m_c a)^2) \\ &\quad + 2b_s \delta x_s (1 + c_s (m_c a)^2) + 4b_{ll} (\delta x_l)^2 \\ &\quad + 2b_{ls} \delta x_l \delta x_s + b_{ss} (\delta x_s)^2\Big]. \end{aligned} \tag{15}$$

We use a constrained fit [34] to this form which allows us to estimate the errors arising from different pieces of the fit. The prior value and width for Δ_{phys} we take as 0.5, with the very broad width of 0.2. Note that we give the discretization errors a scale of m_c. The prior value and width that we take on the c_n parameters is 0.0(2), estimating v^2/c^2 for the c quark inside the D_s to be 0.2. c_1, which multiplies the a^2 errors, is a factor of α_s smaller from the arguments above so we take the prior for c_1 to be 0.00(6). The b parameters multiplying the linear sea-quark mass dependence are taken to have prior values and widths of 0.00(7). The size of the prior width here is set by the fact that the dependence of Δ on the valence light quark mass inside the D_s is known from a comparison of D and D_s. This would give a slope with valence mass, in units of the strange mass, of 0.2. Sea-quark mass effects are a factor of at least 3 smaller than valence mass effects in gold-plated quantities, so we take a prior width of 0.07. By the same reasoning we allow the b parameters multiplying the quadratic dependence to be as large as $(0.2)^2/3$, i.e. we take the prior on these parameters to be 0.000(13).

The extrapolated result at the physical point, Δ_{phys} from the fit above is 0.4753(22) MeV with a χ^2/dof of 0.2 for 11 degrees of freedom. We fit all of the data including the two volumes for the coarse lattices, sets 4 and 5. Missing out set 5 makes no appreciable difference to the result. Modifications to the fit form above also do not change this number significantly. Here we itemize the effect of some of them:

(i) changing the prior on all c_i (including c_1) to 0.0(5) changes Δ_{phys} 0.4σ and increases the error by 20

(ii) adding two extra powers of a^2 into the sum on j in Eq. (15) (i.e. using 6 terms instead of 4) does not change Δ_{phys} or the error at all. The same is true for subtracting two powers of a^2 (i.e. using 2 terms instead of 4).

(iii) adding extra discretization errors into the sea-quark mass dependence (i.e. a term proportional to $(m_c a)^4$ in each of the terms linear in δx_l and δx_s and a term proportional to $(m_c a)^2$ in each of the quadratic terms) makes no difference at all.

(iv) missing out the sea-quark mass dependence altogether makes no difference to Δ_{phys} but increases the χ^2 value to 0.33.

(v) changing all the δx values by 10% in either direction makes no appreciable difference, nor does changing

them within their error bars on, for example, the ultrafine or fine lattices.

(vi) missing out the very coarse lattice results makes no difference; missing out the very coarse and the coarse shifts $\Delta_{\rm phys}$ by 0.4σ (1 MeV), and increases the error to 3 MeV as χ^2 drops to 0.1.

(vii) missing out the ultrafine result shifts $\Delta_{\rm phys}$ by 0.2σ (0.5 MeV) and increases the error to 3 MeV.

Figure 6 shows the results plotted against the square of the lattice spacing along with the fitted curve above, taken at the physical sea-quark mass values (i.e. $\delta x_l = \delta x_s = 0$). The value plotted on the y-axis is m_{D_s} itself, generated by adding $m_{\eta_c}/2 = 1.4925$ GeV to Δ. The result at $a = 0$ is then the value of the D_s mass in a world without electromagnetism. To compare to experiment we need to estimate and add in the effect of the electromagnetic repulsion between the positively charged quark and antiquark inside the D_s. To do this we compare experimental masses for the D^+, D^0, D_s, B^+, B^0 and B_s to a phenomenological formula allowing for electromagnetic effects proportional to the product of quark and antiquark electric charges inside the meson as well as the square of the electromagnetic charge on the light quark. This latter term is a self-energy effect, not needed for the heavy quarks because it will cancel in all the differences taken (and therefore is absorbed into the heavy quark mass). In comparing charged and neutral mesons containing u and d quarks we must allow for the mass difference between u and d quarks. Then we can write [39]:

$$M(Q,q) = M_{\rm sim}(Q,q) + Ae_q e_Q + Be_q^2 + C(m_q - m_l) \quad (16)$$

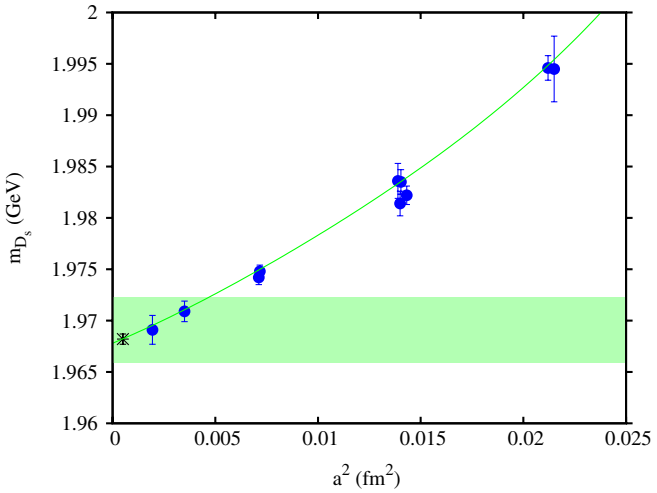

FIG. 6 (color online). Results for the mass of the D_s meson tuned to the correct valence c and s mass on each ensemble from Table IV as a function of the square of the lattice spacing. The line shows the result of the fit described by Eq. (15), taken at the physical values for the sea-quark masses. The shaded band gives our final result adjusted for electromagnetic effects and with the full error as described in the text. The black burst gives the experimental result.

where $M_{\rm sim}$ is the mass of the meson in the absence of electromagnetism and with $m_u = m_d$. If we take experimental results for the meson masses above along with $m_s/m_l = 27.2$ and $m_u/m_d = 0.42$ we obtain $A \approx 4$ MeV, $B \approx 3$ MeV and $Cm_s \approx 100$ MeV. The latter quantity differs by 10% between D and B mesons, indicating $1/m_Q$ effects at this level that we ignore here. The resulting electromagnetic shift for the D_s is then 1.3 (7) MeV, where we take an error of 50% on the shift, safely encompassing $1/m_Q$ effects and other limitations of this model. Adding 1.3 MeV to our fit result gives the shaded band in Fig. 6, where we now include our full error of 3.2 MeV. The full error budget is discussed below.

Figure 7 shows the sea-quark mass dependence of our results plotted against δx_l. The fitted curves are those from Eq. (15). For each group of ensembles we use the lattice spacing value from the ensemble with lightest sea-quark mass to plot the fit curve. No significant dependence on δx_l or δx_s is evident.

Table V shows the complete error budget for m_{D_s} from our calculation. The error of 2.2 MeV from our fit to Δ above includes the effect of statistical errors (including

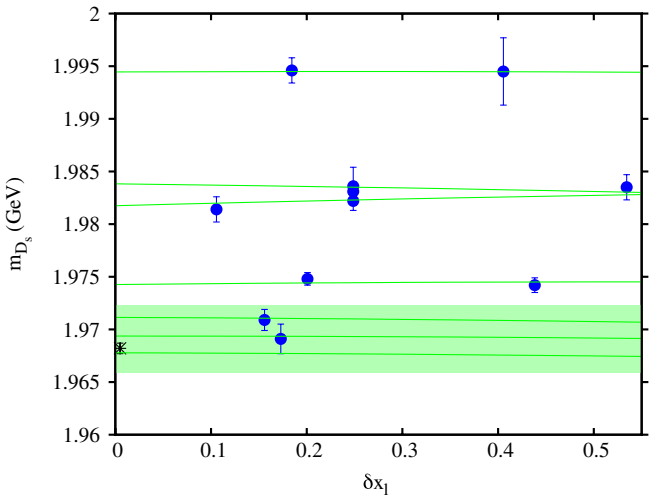

FIG. 7 (color online). Results for the mass of the D_s meson tuned to the correct valence c and s mass on each ensemble from Table IV as a function of the difference between the sea light quark mass and the physical value scaled by the physical strange quark mass (i.e. the parameter δx_l). The results are clearly separated by their lattice spacing value with very coarse at the top and ultrafine at the bottom. The lines show the result of the fit described by Eq. (15), taken at the value of the sea strange quark mass (δx_s) and using the lattice spacing value corresponding to the ensemble with smallest δx_l in that group. The results on the coarse lattices at $\delta x_l = 0.25$ include numbers at two different values of δx_s as well as at two different volumes. This gives an idea of the spread in results from these effects. The lowest line is the fit curve in δx_l at $a = 0$ and $\delta x_s = 0$. The shaded band gives our final result adjusted for electromagnetic effects and with the full error as described in the text. The black burst gives the experimental result.

TABLE V. Full error budget for m_{D_s}, f_{D_s} and f_{η_c} given as a percentage of the final fitted value. Note that in the case of f_{η_c} the top six errors are those to be considered for a lattice QCD calculation that matches this one. As discussed in the text, the bottom three errors are included for completeness.

Error	m_{D_s}	f_{D_s}	f_{η_c}
statistical/valence tuning	0.094%	0.57%	0.45%
r_1/a	0.025%	0.15%	0.16%
r_1	0.051%	0.57%	0.27%
a^2 extrapoln	0.044%	0.40%	0.24%
$m_{q,\mathrm{sea}}$ extrapoln	0.048%	0.34%	0.09%
finite volume	0%	0.10%	0%
m_{η_s}	0.056%	0.13%	-
em effects in D_s	0.036%	0.10%	-
em and annihln in m_{η_c}	0.076%	0.00%	0.05%
em effects in η_c	-	-	0.40%
missing c in sea	0.01%	0%	0.01%
Total	0.16%	1.0%	0.6% (top 6)

valence mass mistuning errors), r_1/a errors and errors arising from the extrapolation in sea-quark masses and lattice spacing. We can separate these errors as described in [32] by working out how the final error changes when any of the inputs to the fit changes and dividing σ^2 into a sum of terms coming from each input:

$$\sigma^2 = \sigma_a^2 + \sigma_b^2 + \ldots. \tag{17}$$

Inputs to the fit include groups of priors associated with pieces of the fit function as well as statistical errors on the data points. Here we streamline the process by calculating explicitly the differential of χ^2 with respect to the inputs and so determining σ_a^2, σ_b^2 etc. directly. The resulting breakdown of errors given in Table V shows them to be dominated by statistical errors.

Additional errors to be included in the error budget are errors that affect the final result in physical units but do not affect the fit above. The first of these is the overall error in the physical value of r_1 of 0.7%. This affects the tuning of all the valence masses but, as described earlier, the effect on Δ is reduced by a factor of 3 because of cancellation between scale shifts and tuning shifts. More precisely we find a 1.0 MeV error on m_{D_s} from the r_1 uncertainty. The effect on Δ of the uncertainty in the physical values of the η_c mass and the η_s mass used in tuning can be judged from Figs. 5 and 4. The error on the η_c mass has negligible effect, again because most of the η_c mass dependence cancels out in Δ. The uncertainty in the η_s mass is not negligible, however, but gives an uncertainty in Δ, which we then transfer to m_{D_s}, of 1.1 MeV. The error on the physical value of the η_c reappears when we reconstruct m_{D_s} from Δ and m_{η_c}. It therefore gives a 1.5 MeV error to m_{D_s} coming from electromagnetic and annihilation effects in the η_c meson mass. The error from electromagnetic effects on the D_s mass itself is 0.7 MeV as described earlier.

The error from the finite volume of the lattices we estimate to be negligible from finite volume chiral perturbation theory. Our lattice results comparing two different volumes (sets 4 and 5) show no significant effect at the level of 0.4

Our lattice calculation includes u, d and s quarks in the sea but no c quarks, although gluon field configurations are now being generated that do include them [40]. In the real world c quarks do appear in the sea and we can estimate the effect of these perturbatively because the c quark mass is relatively heavy, i.e. larger than typical momenta appearing inside the mesons we are discussing. The effect of a massive quark loop in the gluon propagator which gives rise to the heavy quark potential is simply to add a correction to the potential which is proportional to a delta function at the origin [41]:

$$V(r) = -\frac{C_f \alpha_s}{r} \to -C_f \alpha_s \left(\frac{1}{r} + \frac{\alpha_s}{10 m_c^2}\,\delta^3(r)\right). \tag{18}$$

Although this additional term is a spin-independent interaction its effects in charmonium can be judged by comparison to that of the hyperfine potential. The hyperfine potential induces a mass splitting of ≈ 120 MeV from a term which has the same δ function form as above but a coefficient 280 ($= 80\pi/(3\alpha_s)$) times as large. Thus we expect the shift of the η_c (and J/ψ) masses caused by the presence of c quarks in the sea to be approximately 0.4 MeV. The D_s meson has much smaller momenta typically inside it and so we expect a much smaller effect from c quarks in the sea on the D_s meson mass. If we set that effect to zero, so that conservatively there is no cancellation of this effect in the quantity Δ, then we obtain an uncertainty in our final D_s mass of 0.2 MeV, or 0.01%.

Our final result for m_{D_s} is then 1.9691(32) GeV to be compared to an experimental result of 1.9685(3) GeV [37].

B. f_{D_s}

The decay constant of the D_s meson is the main result from this paper. Having discussed in detail the tests that can be successfully done of the D_s mass, we now discuss the analysis of the decay constant.

Table III gives the raw results for the decay constant on the 11 different ensembles we have studied. As for m_{D_s} it is important to be able to understand the dependence of f_{D_s} on the valence c and s masses and to tune the result on each ensemble to the physical values for these masses. As described above, this corresponds to tuning them to physical values of the η_c and η_s meson masses. Figures 8 and 9 show the dependence of f_{D_s} on these meson masses on very coarse, coarse and fine lattices. Again we are using results somewhat above the physical values for the η_s and η_c masses to extract the dependence which will then allow us to tune accurately our results that are much closer to the physical values. As expected, the dependence on $m_{\eta_s}^2 \equiv m_s$ is linear and the slope does not change with lattice

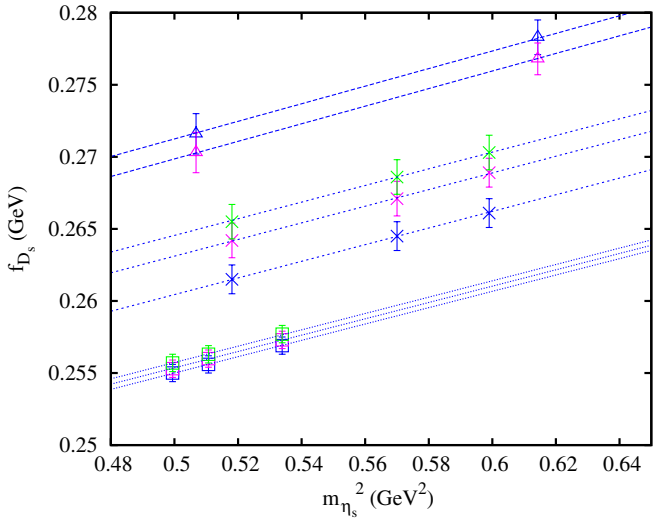

FIG. 8 (color online). Results for the decay constant of the D_s meson as a function of the square of the η_s meson mass, acting as a proxy for the strange quark mass. Results are for a range of different quark masses around the masses of the c and s quark masses on very coarse set 1 (triangles), coarse set 4 (crosses) and fine set 7 (squares). The lines are fits to the results for each ensemble allowing linear terms in $m^2_{\eta_s}$ and m_{η_c}. Here the lines join points for a fixed c quark mass. See Fig. 9 for the equivalent as a function of m_{η_c}.

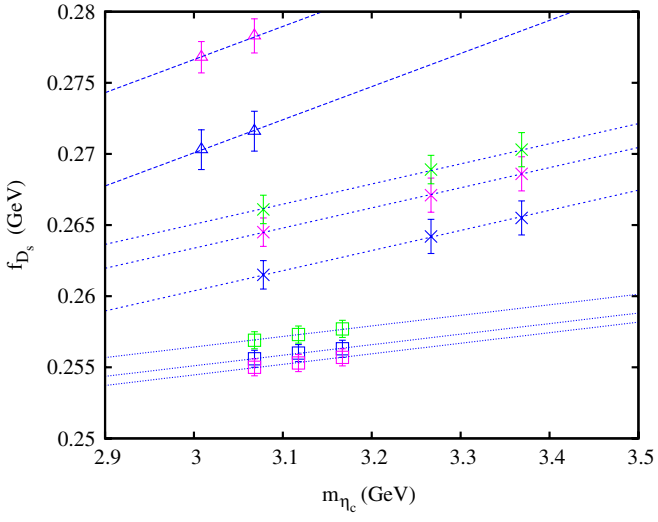

FIG. 9 (color online). Results for the decay constant of the D_s meson as a function of the η_c meson mass, acting as a proxy for the charm quark mass. Results are for a range of different quark masses around the masses of the c and s quark masses on very coarse set 1 (triangles), coarse set 4 (crosses) and fine set 7 (squares). The lines are fits to the results for each ensemble allowing linear terms in $m^2_{\eta_s}$ and m_{η_c}. Here the lines join points for a fixed s quark mass. See Fig. 8 for the equivalent as a function of $m^2_{\eta_s}$.

spacing. The value of the slope, 0.06 GeV^{-1} can be compared to the change in f_{D_q} expected from $q = s$ to $q = l$ [3]. This corresponds to a somewhat larger slope of 0.09 GeV^{-1} but is over a much larger range where nonlinear effects may appear. The slope of f_{D_s} against m_{η_c} falls from very coarse to fine lattices. This has interesting implications for the behavior of the heavy-strange meson decay constant as a function of heavy quark mass. It is clear from the study of the η_s and D_s mesons that the decay constant increases as the "heavy" quark mass is increased from m_s to m_c. However, above m_c the behavior is less clear because lattice QCD calculations have so far not been accurate enough to distinguish clearly what is happening to within 5–10% errors. There are known to be large corrections to the $1/\sqrt{m_Q}$ behavior expected from HQET because f_{D_s} and f_{B_S} are not very different [42]. This is consistent with a slope against heavy quark mass for f_{D_s} that tends to zero. It is clear that understanding this dependence also requires good control of discretization errors.

Again we use the dependence shown in these plots to make small tuning shifts to the values of f_{D_s} on each ensemble so that they correspond to the correct result for $m_{\eta_c} = 2.985$ GeV and $m_{\eta_s} = 0.6858$ GeV. Table IV gives the tuned values on each ensemble. Because the statistical errors are about twice as large for f_{D_s} as for Δ and the dependence on m_{η_c} and m_{η_s} is smaller, the tuning shifts, and the errors from them, are very much less than the statistical errors on all ensembles. Even on set 2 the shift from mistuning is only 1σ. The error in f_{D_s} from the uncertainty in r_1/a is only slightly reduced over its naive value from cancellations. It is also much smaller than the statistical error everywhere. It is given as the second error in Table IV.

Again it is clear from Table IV that the sea-quark mass dependence of the results is smaller than our 1–2 MeV statistical errors, but the lattice spacing dependence is not. We therefore fit the sea-quark mass dependence with a relatively simple form that allows an error for what little dependence there is to be included in the final extrapolated value at the physical point. For the lattice spacing dependence we include relatively high order terms to make sure that a sufficiently large error is included in the final extrapolated value for this dependence. The fit form is the same as that used for Δ:

$$
\begin{aligned}
&f_{D_s}(a, \delta x_l, \delta x_s) \\
&= f_{D_s,\mathrm{phys}}\Big[1 + \sum_{j=1}^{4} c_j (m_c a)^{2j} + 2b_l \delta x_l (1 + c_b (m_c a)^2) \\
&\quad + 2b_s \delta x_s (1 + c_s (m_c a)^2) + 4b_{ll} (\delta x_l)^2 \\
&\quad + 2b_{ls} \delta x_l \delta x_s + b_{ss} (\delta x_s)^2\Big]. \qquad (19)
\end{aligned}
$$

We take the same prior values and widths as before except that for $f_{D_s,\mathrm{phys}}$ we take to be 0.25(10).

The extrapolated result at the physical point, $f_{D_s,\mathrm{phys}}$ is 0.2480(19) GeV with a χ^2/dof of 0.2 for 11 degrees of freedom. The fit is robust to changes in the fitting function:

(i) changing the prior on all the c_i (including c_1) to 0.0 (5) changes $f_{D_s,\mathrm{phys}}$ by 0.8σ and increases the error by 30%.

(ii) adding or subtracting two powers of a^2 into the sum on j in Eq. (19) does not change $f_{D_s,\mathrm{phys}}$ or its error.

(iii) adding an extra power of discretization errors into both the linear and quadratic sea-quark mass dependent terms makes no difference.

(iv) missing out the sea-quark mass dependence altogether changes $f_{D_s,\mathrm{phys}}$ by 0.2σ but increases the χ^2 value to 0.3.

(v) Changing all the δx values by 10% in either direction makes no appreciable difference, nor does changing them within their error bars on, for example, the ultrafine or fine lattices.

(vi) missing out the very coarse lattice results does not change $f_{D_s,\mathrm{phys}}$; missing out the very coarse and the coarse shifts $f_{D_s,\mathrm{phys}}$ by 0.3σ (1 MeV).

(vii) missing out the ultrafine result shifts $f_{D_s,\mathrm{phys}}$ by 0.4σ (1 MeV).

Figure 10 shows the results plotted against the square of the lattice spacing. The line is the fit curve for the physical sea-quark mass values (i.e. $\delta x_l = \delta x_s = 0$). The shaded band is then the final physical result including the full error of 1.0% (2.5 MeV), to be discussed below and broken down into its component parts in Table V.

We construct the error budget as before, separating the error of 1.9 MeV resulting from the extrapolation to the physical point into its components of statistical error, r_1/a error and errors from extrapolation in the lattice spacing and in the sea-quark masses. Here the contributions from statistical errors and the different extrapolation errors are comparable.

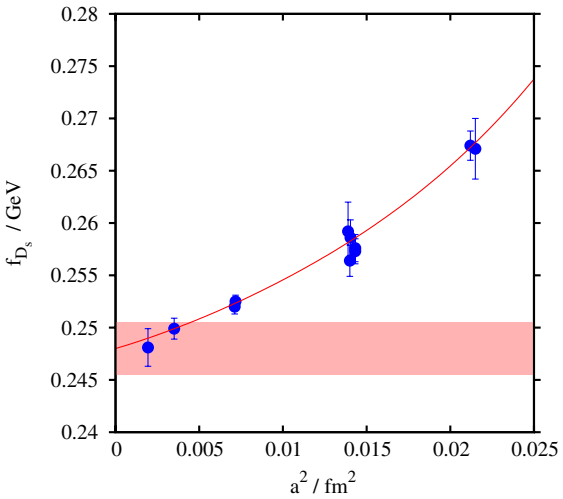

FIG. 10 (color online). Results for the D_s decay constant tuned to the correct c and s mass on each ensemble as a function of the square of the lattice spacing. The line shows the result of the fit at the physical value for the sea-quark masses, as described in the text. The shaded band gives our final result with the full error bar as described in the text.

The error in the physical value of r_1 is 0.7%. This becomes a 0.6% error in f_{D_s} when the effects of r_1 on shifting the value of m_{η_s} are taken into account. The effect of the 0.6% uncertainty in the physical value of m_{η_s} can similarly be estimated from the dependence of f_{D_s} on the η_s mass at 0.1%. The uncertainty in f_{D_s} from the uncertainty in the value of the η_c mass is negligible. The error from working on a finite spatial volume instead of infinite volume is estimated at 0.1% from comparing finite and infinite volume chiral perturbation theory. It is clear from our results (see Table III) that we see no significant volume dependence within our 0.5% statistical errors, which is in agreement with chiral perturbation theory, but that provides a stronger constraint.

The size of electromagnetic effects inside the D_s can be bounded by the size of these effects on the η_c. By allowing for an electromagnetic contribution to the heavy quark potential we estimate that f_{η_c} could be increased by up to 0.4% by these effects. Since the D_s has one quark of half the electromagnetic charge and is also much larger, so less sensitive to short-distance electromagnetic effects, we conservatively take an error of 0.1% from internal electromagnetic effects [43].

The error resulting from missing c quarks in the sea can also be bounded by the size of such effects on f_{η_c}. In Sec. III A we discussed a comparison between the hyperfine potential in charmonium and that induced by adding c quarks in the sea. The hyperfine potential causes the difference between $f_{J/\psi}$ and f_{η_c}, which we will see in the next section is very small, 3%. The c-in-the-sea potential is 280 times smaller and so will produce a completely negligible effect on f_{η_c} and therefore also on f_{D_s}.

Figure 11 shows the results for f_{D_s} as a function of the sea light quark mass, normalized to the strange mass as in Eq. (A3). The lines show the fitted curves at the appropriate values of lattice spacing and sea strange quark mass, along with the final physical curve and final result with error band. No significant dependence on sea-quark masses is seen.

Our final result for f_{D_s} is 0.2480(25) GeV, to be compared to the October 2010 average from the Heavy Flavor Averaging Group of 0.2573(53) GeV [25].

C. f_{η_c}

Here we study the remaining independent quantity that can be extracted from the pseudoscalar correlators calculated here, the decay constant of the η_c meson. Although this cannot be directly related to any process measurable in experiment, it can be compared between lattice QCD

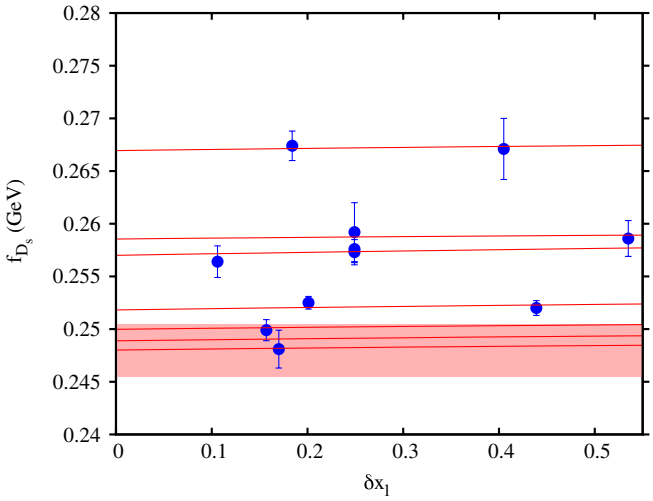

FIG. 11 (color online). Results for the decay constant of the D_s meson tuned to the correct valence c and s mass on each ensemble from Table IV as a function of the difference between the sea light quark mass and the physical value scaled by the physical strange quark mass (i.e. the parameter δx_l). The results are clearly separated by their lattice spacing value with very coarse at the top and ultrafine at the bottom. The lines show the result of the fit described by Eq. (19), taken at the value of the sea strange quark mass (δx_s) and using the lattice spacing value corresponding to the ensemble with smallest δx_l in that group. The results on the coarse lattices at $\delta x_l = 0.25$ include numbers at two different values of δx_s as well as at two different volumes. This gives an idea of the spread in results from these effects. The lowest line is the fit curve in δx_l at $a = 0$ and $\delta x_s = 0$. The shaded red band gives our final result with the full error as described in the text.

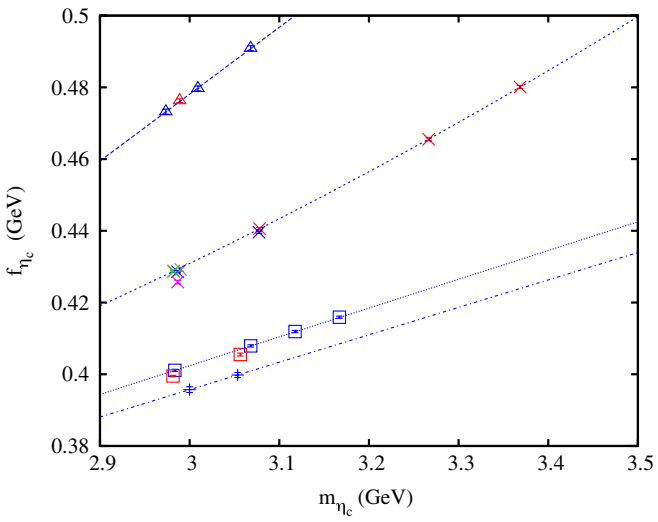

FIG. 12 (color online). Results for the η_c decay constant as a function of the η_c mass for the different ensembles in Table I. As in Fig. 1, very coarse ensembles are triangles; coarse, crosses; fine, squares; superfine, pluses. Errors shown are statistical only. Results for heavier sea u/d quark masses at each lattice spacing are in red, lighter ones are in blue. On the coarse lattices the very heavy sea masses of set 6 are in pink, the lighter strange sea mass of set 7 in grey and the large volume results on set 5 are in green, on top of the result from set 4. The lines are fits to the results for one ensemble at each lattice spacing allowing linear and quadratic terms in m_{η_c}.

calculations using different formalisms for the c quarks. Since we have particularly accurate results here, we give a value for f_{η_c} that others can use to test their formalisms against.

The raw results for f_{η_c} on each ensemble are given in Table II. Since the η_c contains only charm quarks we have only to plot f_{η_c} against m_{η_c} to interpolate to the correct point on each ensemble. Because this is simpler than having to separate the dependence on two masses, as was done for the D_s, we can plot the results from many more of the ensembles. Figure 12 shows the results. As expected, the dependence is linear (we allowed for quadratic terms in the fit, but these were small) but with a slope that depends on the lattice spacing. The figure also emphasizes how little sea-quark mass dependence there is, in line with the evidence from Fig. 1. Some is visible above our very small statistical errors on the coarse and fine ensembles, however.

Again we use the dependence shown in Fig. 12 to make small tuning shifts to the values of f_{η_c} on each ensemble so that they correspond to the correct result for $m_{\eta_c} = 2.985$ GeV. Table IV gives these tuned values. The statistical/tuning errors are small but the r_1/a errors are even smaller because of cancellation when the retuning is done on changing the lattice spacing. Once again the lattice spacing dependence is the most striking feature of these results.

We fit the tuned values to the same functional form as used for m_{D_s} (Eq. (15)) and f_{D_s} (Eq. (19)). We take the same prior values and widths for the parameters except that for the physical value of f_{η_c}, $f_{\eta_c,\mathrm{phys}}$ we take 0.4(2) and for the coefficients, c_i, for the discretization errors we take 0.0 (3), since v^2 for a c quark is expected to be somewhat higher than in a D_s.

The extrapolated value at the physical point, $f_{\eta_c,\mathrm{phys}}$, is 0.3947(20) GeV with a χ^2/dof of 0.3 for 11 degrees of freedom. Once again we tested how robust the fit was:

(i) changing the prior on all the c_i (including c_1) to 0.0 (8) changes $f_{\eta_c,\mathrm{phys}}$ by 0.5σ (1 MeV) and increases the error by 40%.

(ii) adding two powers of a^2 into the sum on j in the fit equation does not change $f_{\eta_c,\mathrm{phys}}$ or its error; subtracting two powers changes $f_{\eta_c,\mathrm{phys}}$ by 0.5σ (1 MeV) and reduces the error by 30%.

(iii) adding an extra power of discretization errors into both the linear and quadratic sea-quark mass dependent terms makes no difference.

(iv) missing out the sea-quark mass dependence altogether does not change $f_{\eta_c,\mathrm{phys}}$ but increases the χ^2 value to 1.

(v) Changing all the δx values by 10% in either direction makes no appreciable difference, nor does changing them within their error bars on, for example, the ultrafine or fine lattices.

(vi) missing out the very coarse lattice results does not change $f_{\eta_c,\mathrm{phys}}$ appreciably; neither does missing out the very coarse and the coarse but the error increases by 50%.

(vii) missing out the ultrafine result shifts $f_{\eta_c,\mathrm{phys}}$ by 1.4σ (2.5 MeV) and increases the error by 40%.

The error budget is constructed as before, estimating the split in the error obtained from the fit into components from statistics, r_1/a and extrapolations in a^2 and the sea-quark masses. In addition the error from the uncertainty in the physical value of r_1 becomes 0.3%, allowing for the cancellation that reduces the sensitivity below the naive 0.7%. The error from finite volume effects we take to be negligible based on the chiral perturbation theory studies of the much larger D_s meson.

As we will discuss in Sec. IV, f_{η_c} is not a quantity that can be compared directly to experiment. We include it here as a calibration point for lattice QCD studies of charm physics. As such, we do not have to include errors arising from effects outside a pure lattice QCD calculation including u, d, and s sea quarks and taking the η_c mass to be 2.985 GeV. Thus in Table V only the top six errors in the final column should be included for such a calculation and the bottom three ignored.

For completeness we discuss other sources of error that may need to be considered if lattice QCD calculations differing in detail from ours are compared to it. The error that arises from the 3 MeV uncertainty in the physical value of the η_c mass can be estimated from the slope of f_{η_c} with m_{η_c} in Fig. 12. This gives an error of 0.05% with f_{η_c} increasing with the value of m_{η_c}. Internal electromagnetic effects inside the η_c will also increase f_{η_c}. In Sec. III B we estimated this effect at 0.4% (but lattice QCD calculations will not typically include electromagnetic effects). The effect of including c quarks in the sea will also be to increase f_{η_c}. In Sec. III B we estimated this as 0.01%, based on a comparison to $f_{J/\psi}$ that will be described in Sec. IV B 3.

Figure 13 shows f_{η_c} against a^2 in fm^2 with the fit curve for the physical sea-quark mass values. The shaded band is the final physical result including the full 0.6% error, i.e. 0.3947(24) GeV.

Figure 14 shows the results for f_{η_c} as a function of the sea light quark mass, normalized to the strange mass as in Eq. (A3). The lines show the fitted curves at the appropriate values of lattice spacing and sea strange quark mass, along with the final physical curve and final result with error band. No significant dependence on sea-quark masses is seen.

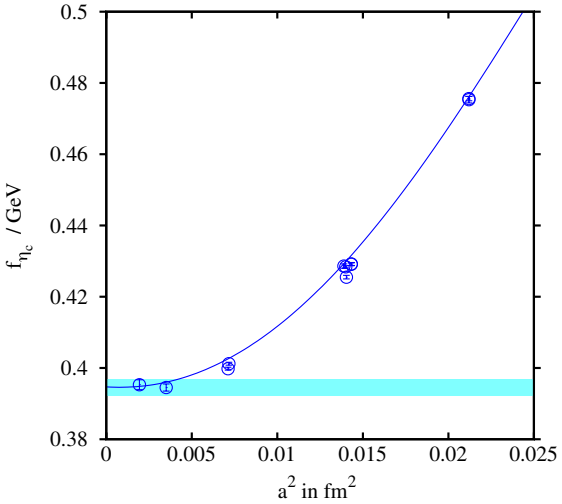

FIG. 13 (color online). Results for the η_c decay constant tuned to the correct c mass on each ensemble as a function of the square of the lattice spacing. The line shows the result of the fit described in the text. The shaded band gives our final result with the full error bar as described in the text.

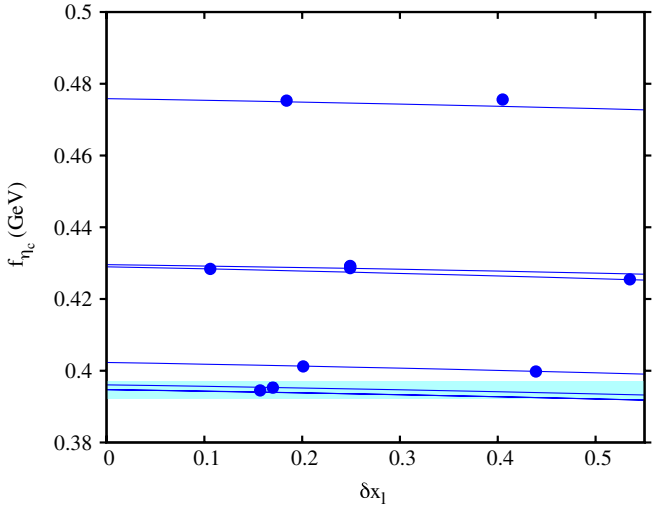

FIG. 14 (color online). Results for the decay constant of the η_c meson tuned to the correct valence c mass on each ensemble from Table IV as a function of the difference between the sea light quark mass and the physical value scaled by the physical strange quark mass (i.e. the parameter δx_l). The results are clearly separated by their lattice spacing value with very coarse at the top and ultrafine at the bottom. The lines show the result of the fit described in the text, taken at the value of the sea strange quark mass (δx_s) and using the lattice spacing value corresponding to the ensemble with smallest δx_l in that group. The results on the coarse lattices at $\delta x_l = 0.25$ include numbers at two different values of δx_s as well as at two different volumes. This gives an idea of the spread in results from these effects. The lowest line is the fit curve in δx_l at $a = 0$ and $\delta x_s = 0$. The shaded blue band gives our final result with the full error as described in the text.

IV. DISCUSSION

A summary of the results from this calculation is then:

$$m_{D_s} = 1.9691(32)\ \text{GeV} \qquad f_{D_s} = 0.2480(25)\ \text{GeV}$$
$$f_{\eta_c} = 0.3947(24)\ \text{GeV}. \tag{20}$$

A. Comparison to our previous results

Our new results improve on our 2007 results [3] in several ways, as described earlier. It is worth discussing the effect of these changes on the final numbers because, particularly in the case of f_{D_s}, the shift from 2007 is significant.

Our 2007 result for m_{D_s} was 1.962(6) GeV obtained from very coarse, coarse and fine ensembles. The lattice spacing was fixed using the quantity r_1 as here, but setting the physical value of r_1 to 0.321(5) fm. The error on m_{D_s} from this uncertainty in r_1 was 0.2% i.e. 4 MeV. Since then we have improved significantly the calibration of the lattice spacing by improving the determination of the physical value of r_1 to 0.3133(23) fm. This has used improved determinations of r_1/a on each ensemble by the MILC Collaboration [31]. The change in the value of r_1 represents 1.5σ and therefore we expect m_{D_s} to change by approximately 6 MeV. In fact the change has been 7 MeV.

Of course the change in r_1 has not been the only change. The lattice spacing values on individual ensembles have moved relative each other with changes in r_1/a values. These have moved furthest on the very coarse set 1, changing by 1% or 2σ, but with some changes of up to 0.5% (1σ) on the coarse ensembles. Values on the fine ensembles have not shifted significantly. The relative shifts change the lattice spacing extrapolation slightly, as does our improved tuning of the charm quark mass (the strange mass was tuned within the chiral extrapolation previously using results for the K and π meson masses). We also have additional determinations of the sea-quark mass dependence. These other effects largely cancel each other, however, in this case. Our new error budget shows an improved error coming from the determination of r_1 and this is the main effect behind the reduction of total error from 0.3% to 0.2%.

Our f_{D_s} result has changed by 2.7% (from 0.2415 (32) GeV) which is a shift of 2σ. From our error budget the change expected from the change in r_1 is 1.5%. Combined with changes in r_1/a and improved tuning, however, results on the fine and very coarse ensembles have changed by up to 2%. This has affected the continuum extrapolation. Sea-quark mass effects, although not significant either now or before, have also changed in the same direction. This has meant that the 0.3% sea-quark mass extrapolation error has added linearly to (some of) the 0.5% continuum extrapolation and the roughly 2% shift, rather than in quadrature.

The ratio f_{D_s}/f_D is not very sensitive to r_1 and so, although we have not yet performed an improved analysis of f_D, we would not expect this ratio to change very much. If we take our previous result for f_{D_s}/f_D, but double the r_1 uncertainty and add it linearly to the a^2 and $m_{u,d}$ extrapolation errors to allow for the behavior seen in f_{D_s}, we would obtain an error of 1.5% on the ratio, giving 1.164 (18). Combined with our new result for f_{D_s} this gives a value for f_D of 0.213(4) GeV, to be compared to a CLEO result of 0.206(9) GeV [13]. We emphasize that our new value for f_D does not result from a new analysis of f_D itself but simply from the change in f_{D_s} given here.

Our 2007 results for f_π and f_K change a little when the new value for r_1 is used. Using the fitting procedure described in the appendices of [35] (but not including the experimental results for f_π and f_K in the fit data), we find $f_\pi = 132(2)$ MeV and $f_K = 159(2)$ MeV which agree within errors with our 2007 results [3] and with experiment [37] to within about 1.5σ.

B. Comparison to other lattice results and to experiment

1. m_{D_s}

As discussed in Sec. III A, the accurate determination of the mass of the D_s meson is an important test of the calculation of f_{D_s}. Our result, 1.9691(32) GeV, is in good agreement with experiment, as shown in Fig. 6. The experimental error is 0.3 MeV [37]. To improve the lattice QCD error of 3 MeV further would require improved statistical errors on the very fine lattices but also improved errors from electromagnetic/η_c annihilation effects that are not currently included in lattice QCD calculations. It is impressive that lattice QCD calculations have reached the point where electromagnetic effects have to be considered in the match to experiment.

Other lattice QCD formalisms for c quarks are not as highly improved as HISQ. They then have more difficulty in handling charmonium and so fix the c quark mass from the D_s. However, we believe that it is still important to check the masses of other mesons containing c quarks as a test of systematic errors. The easiest quantity to compare is the one defined earlier as $\Delta = m_{D_s} - m_{\eta_c}/2$, the difference in binding energy between charmonium and D_s. Our result for this is plotted in Fig. 15. A variant of Δ was recently calculated using the Fermilab heavy quark formalism for c quarks, combining this with light asqtad quarks on the MILC very coarse, coarse and fine ensembles [44]. The c mass is fixed from the energy-momentum relation for the D_s meson (because the energy at zero momentum is not equal to the mass), which leads to sizeable statistical errors in the tuning process, growing with heavy quark mass [45]. Typically the ''kinetic mass'' for the D_s is obtained to 2%. The Fermilab lattice/MILC collaborations quote a result for $\Delta' = m(\bar{D}_s) - m(\overline{1S})/2$ of $0.529 \pm 7\,^{+12}_{-0}$

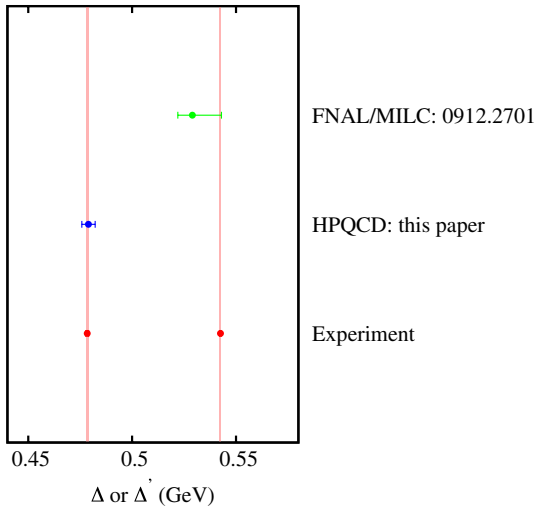

FIG. 15 (color online). Summary of full lattice QCD results for the difference of binding energy between charm-strange and charmonium states. Δ uses pseudoscalar mesons D_s and η_c and compares the result from this paper to experiment, given by the appropriate red point and shaded band). Δ' uses a spin-average of the pseudoscalar and vector states and compares the result from the Fermilab Lattice/MILC Collaborations to experiment. Our result corresponds to the complete error budget given in Table V and is corrected for missing electromagnetic effects. The Fermilab Lattice/MILC result includes both errors given in [45] but has not been corrected for missing electromagnetic effects.

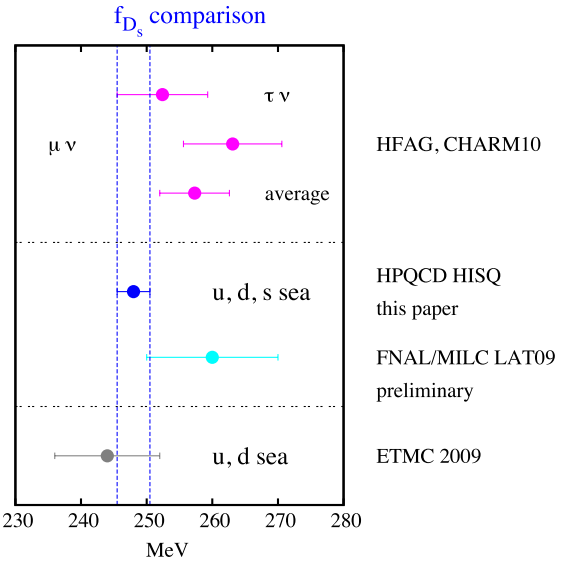

FIG. 16 (color online). Comparison of the result from this paper for the D_s decay constant with those from other lattice QCD calculations that include the effect of sea quarks. The Fermilab Lattice/MILC result is a preliminary one but also includes the effects of u, d and s quarks in the sea. The ETMC result includes only u and d quarks in the sea. We show also a recent average of experimental results from the Heavy Flavor Averaging Group [25] and two separate averages over the $\mu\nu$ and $\tau\nu$ channels. Experimental results for f_{D_s} convert the leptonic decay rate to a decay constant using Eq. (21) and using an input value for V_{cs} (see text).

with a partial error budget [44]. Here $\bar{D}_s$ indicates the spin-average mass of the D_s and the D_s^* and $m(\overline{1S})$ is the spin average of the masses of the J/ψ and the η_c. The spin average is used to reduce their discretization error from spin-dependent terms, but the D_s^* does have a strong decay mode, albeit Zweig-suppressed, that will lead to an additional systematic error in the lattice QCD calculation. The first error given above is from statistics and extrapolation uncertainties and the second from the physical value of r_1 which they take as $0.318\,^{+0.000}_{-0.007}$ fm. The Fermilab Lattice/MILC result agrees with experiment and is plotted in Fig. 15 for comparison to our result for Δ. More detailed comparison between the results needs improved accuracy for those from the Fermilab formalism.

2. f_{D_s}

Figure 16 compares the result for the D_s decay constant from this paper to other lattice QCD calculations that include the effect of sea quarks. The Fermilab Lattice/MILC result of 260(10) MeV is a preliminary one from a conference presentation [46], updated from their original 2005 calculation [7] in a number of ways but including an update of the physical value of the parameter r_1 used to set the lattice spacing as we have done here. Their calculation uses MILC gluon field configurations as we do, but at the three coarsest lattice spacing values that we have used. The Fermilab formalism for c quarks is combined with the asqtad formalism for the s quarks. As explained above the c quark mass is tuned from the dispersion relation for D_s mesons. In the Fermilab formalism there is no PCAC relation and so the temporal axial current operator that annihilates the D_s in its leptonic decay (Eq. (11)) must be renormalized to match the continuum current operator that couples to the W. This is done by a perturbative calculation to $\mathcal{O}(\alpha_s)$ after taking a ratio to vector current operators. The systematic uncertainty from this approach is in principle $\mathcal{O}(\alpha_s^2)$ ($\approx 5\%$), but it is argued in [46,47] that a significantly smaller (1.4% + 0.3%) error be used which is the square of the one-loop contribution. It would be useful to test this on a calculation such as f_K where the result is well-known [48]. With relativistic formalisms such as the HISQ formalism used here and the twisted mass formalism to be discussed below, the existence of the PCAC relation means that the issue of renormalization does not arise. Also in both cases, f_K can be calculated as well as f_{D_s} as a test of the error analysis.

Figure 16 also includes the result 244(8) MeV from the European Twisted Mass Collaboration [49] using the twisted mass formalism for all of the quarks. This formalism is an improved version of the Wilson formalism with discretization errors starting at $\mathcal{O}(a^2)$, somewhat worse than the $\mathcal{O}(\alpha_s a^2)$ for HISQ, but also having a partially

conserved axial current so no renormalization issues. ETMC include only the effect of u and d quarks in the sea, however, and it is not clear what systematic error to take for missing s quarks that are there in the real world. We cannot use perturbative arguments, as we have done here to account for the missing c quarks in the sea. ETMC are now improving their calculations to include both s and c sea quarks [50].

The experimental results shown on Fig. 16 are the October 2010 averages from the Heavy Flavor Averaging Group [25], using recent CLEO [21–23], *BABAR* [24,26] and Belle [15] results from measurement of the $D_s \to \mu\nu$ and $D_s \to \tau\nu$ decay rates. To determine f_{D_s} from experiment the measured leptonic branching fraction, corrected for electromagnetic radiation [43], is used in

$$f_{D_s} = \frac{1}{G_F |V_{cs}| m_l (1 - m_l^2/m_{D_s}^2)} \sqrt{\frac{8\pi \mathcal{B}(D_s \to l\nu)}{m_{D_s} \tau_{D_s}}}. \quad (21)$$

A value for V_{cs} must be assumed. In the past $V_{cs} = V_{ud}$ has often been taken (see, for example, [21]), assuming 2×2 CKM unitarity. HFAG take the 2010 Particle Data Tables result for V_{cs} (0.97345(16)) from a full CKM matrix unitarity fit [25,37]. These two alternatives for V_{cs} differ at the level of 0.1% which is irrelevant here.

It is clear from Fig. 16 that there is no longer any significant "f_{D_s} puzzle" [51] since the discrepancy between our lattice QCD result and the world average of experiment (257.3(5.3) MeV) is 1.6σ. The average of experimental results in the $\tau\nu$ channel (252.4(6.9) MeV) and our value agree very well. This is emphasized further in Fig. 17 where the most accurate recent experimental results are individually compared to our value for f_{D_s}, and all except one disagree by less than 1σ.

Things have now changed quite significantly since the summer of 2008 when the most accurate experimental result for f_{D_s} was 267.9(9.1) MeV [16] and the most accurate lattice QCD result was 241(3) MeV [3,17], differing by almost 3σ. The experimental average moved down 5% (1.5σ) in early 2010 but has since moved up 1% to the new world average value and the lattice result has moved up 3% (2.3σ). The discrepancy between experiment and lattice QCD is now only 4% (1.6σ) and the experimental error is now reduced to only twice that of the lattice QCD error. This marks significant effort both experimentally and theoretically on this quantity to understand and pin down the original discrepancy. Figure 18 shows the history of f_{D_s} from experiment and lattice QCD since the first full lattice QCD calculation of 2005.

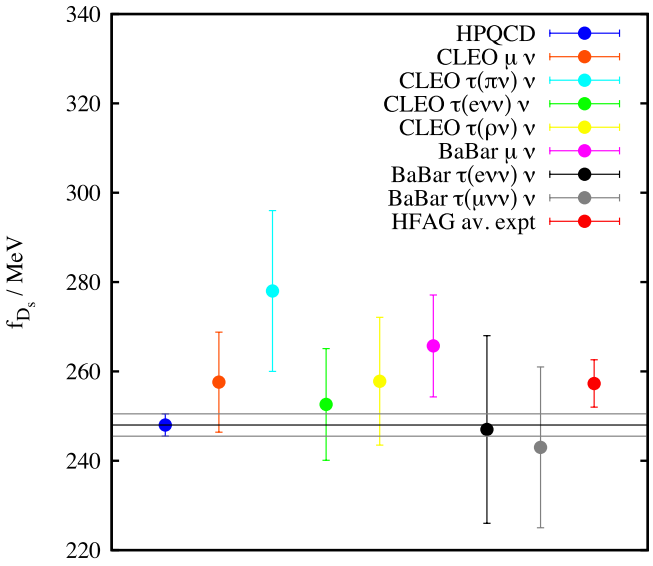

FIG. 17 (color online). Comparison of our new result for the D_s decay constant with recent experimental results from CLEO [21–23] and *BABAR* [26]. These are derived from leptonic decay modes of the D_s in various channels, and using Eq. (21) with an input value for V_{cs} (see text). The CLEO numbers are taken from the compilation in [23], using consistent values for V_{cs}, m_{D_s} and τ_{D_s} and so differ slightly from the historical numbers in Fig. 18. We also include the HFAG 2010 world average for experiment [25].

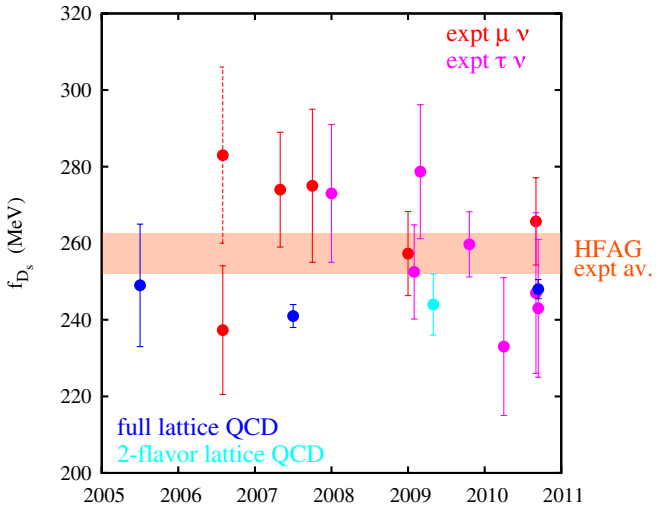

FIG. 18 (color online). Values for f_{D_s} from experiment and from lattice QCD since 2005, excluding results from conference proceedings. Later results from a given collaboration and process supersede the earlier ones. Experimental results are divided into those from the $\mu\nu$ channel [11,12,15,21,26] (in red) and those from the $\tau\nu$ channel [11,14,21–24,26] (in several τ decay modes, in pink). The HFAG October 2010 world average for experiment [25] is included as a light orange band. Note that the leftmost red point (from *BABAR* [12]) appears with dashed error bars—the lower value with solid error bars is the result adjusted by HFAG [65], although this number is not now included in the HFAG average. Lattice QCD points are in dark blue for full QCD [3,7]—the rightmost point is from this paper. The light blue point is from ETMC [49] including only u and d in the sea.

3. f_{η_c}

As stated earlier, there is no direct comparison possible between lattice results for f_{η_c} and experiment because the η_c does not annihilate to a W boson or other particle that would couple directly to the temporal axial current. The high accuracy of our results is therefore useful only to provide a comparison point for other lattice QCD calculations. No result of comparable accuracy is available from any other charm quark formalism as yet and including the effect of sea quarks. ETMC [52] quote a preliminary result of 379(29) MeV for f_{η_c} including u and d quarks in the sea only and tuning the c mass from the mass of the J/ψ (i.e. this analysis is not directly linked to their D_s analysis, as ours is). Future lattice charmonium calculations using different formalisms (for example [53] or [54]) can use our result as a benchmark point to check renormalization or discretization effects because f_{η_c} is a very simple quantity to calculate.

Although direct comparisons with experiment do not exist, various comparisons that rely on approximation schemes, principally potential models, can be made. In a potential model the decay constant of an S-wave state is related to the wave function at the origin, $\psi(0)$, by $\psi(0) = f\sqrt{M/12}$, where M is the meson mass and f its decay constant. This relationship is only correct up to relativistic and radiative corrections, which for the η_c could be sizeable (at the level of 30%). Using this same potential model approach the leading term in the decay width for $\eta_c \to \gamma\gamma$ can be written as [55]

$$\Gamma(\eta_c \to \gamma\gamma) = \frac{12\pi e_c^4 \alpha^2 |\psi(0)|^2}{m_c^2}. \tag{22}$$

Here the c quark has electromagnetic charge e_c (in units of e), mass m_c and α is the electromagnetic coupling constant. This formula has radiative and relativistic corrections at the next order. The decay width is only poorly known for the η_c with the PDG estimate given as 7.2(2.1) keV [37]. Substituting the decay constant into the formula and taking $m_c = M_{\eta_c}/2$, justifiable at this order, gives $f_{\eta_c} = 0.4(1)$ GeV, where only the large error from experiment is shown. Alternatively one may extract f_{η_c} from B decays to $\eta_c K$ using the factorization approximation. CLEO obtain $f_{\eta_c} = 0.335(75)$ GeV [56].

A more useful experimental result to compare to our decay constant is probably the decay constant of the J/ψ. Because the J/ψ can annihilate to a photon (seen as two leptons in the final state) through the vector current there is an exact relationship between the decay width and the decay constant of the vector particle defined in an analogous way to that for the pseudoscalar meson by

$$\sum_i < 0|\bar{\psi}\gamma_i\psi|V_i > /3 = f_V m_V. \tag{23}$$

This decay constant can also be calculated in lattice QCD [32]. Work is in progress and results will be given elsewhere. The relationship between decay width and decay constant for the process $V_h \to e^+e^-$ is then

$$\Gamma(V_h \to e^+e^-) = \frac{4\pi}{3}\alpha_{\rm QED}^2 e_Q^2 \frac{f_V^2}{m_V}. \tag{24}$$

The experimental results [37] give $f_{J/\psi} = 407(5)$ MeV using $1/\alpha_{\rm QED}(m_c) = 134$ [57]. Thus 1% accurate results for this decay constant are available from experiment, and can be used to test lattice QCD. In a potential model vector and pseudoscalar values of $\psi(0)$ should differ only by relativistic corrections, since this is a spin-dependent effect which appears first at subleading order in the velocity-squared of the heavy quark. Thus we would expect our results for the pseudoscalar decay constant to be fairly close to those for the vector. It is hard to make this statement quantitative however because, even if the difference in $\psi(0)$ values of vector and pseudoscalar were accurately pinned down, the relationship of $\psi(0)$ to the decay constant could have sizeable radiative and relativistic corrections.

Our result for f_{η_c}, 0.3947(24) GeV, is in fact very close to the experimental result for $f_{J/\psi}$, only differing by 3% (2σ). This is somewhat surprising, given naive potential model arguments. Accurate lattice QCD studies in bottomonium will show whether this is a coincidence at the charm mass or a more general feature.

V. CONCLUSIONS

In this paper we have updated our 2007 result for the mass and decay constant of the D_s meson [3] to incorporate a new more accurate calibration of the energy scale in lattice QCD. We have also included results at two finer values of the lattice spacing so we now cover a range of lattice spacing values from 0.15 fm down to 0.044 fm for improved determination of the continuum limit. Our results for m_{D_s} and f_{D_s} increase as a result of this calibration. m_{D_s} is in excellent agreement with experiment with a reduced (3 MeV) error to give 1.9691(32) GeV. Our result for f_{D_s} has increased significantly to 0.2480(25) GeV. This, along with recent movement of the experimental results, means that the "f_{D_s} puzzle" is essentially solved: there is no longer significant disagreement between theory and experiment for this quantity. The experimental error is double the theoretical error, however, and improved experimental results from BESIII aim to obtain a 1% on f_{D_s} [58]. The lattice QCD error could be further reduced by improved statistical accuracy on the very fine lattices.

Instead of assuming a value for V_{cs} to obtain an experimental result for f_{D_s} to compare to lattice QCD we can combine our result for f_{D_s} with the experimental leptonic branching fraction to give a direct determination of V_{cs}. To do this we take the HFAG determination [25] of the world average leptonic branching fractions for the D_s to $\mu\nu$ and $\tau\nu$ of 0.590(33)% and 5.29(28)%, respectively, our result for f_{D_s} and

$$V_{cs} = \frac{1}{G_F f_{D_s} m_l (1 - m_l^2/m_{D_s}^2)} \sqrt{\frac{8\pi \mathcal{B}(D_s \to l\nu)}{m_{D_s} \tau_{D_s}}}. \quad (25)$$

This gives results for V_{cs} of

$$V_{cs} = 1.033(31), \qquad D_s \to \mu\nu$$
$$= 0.990(28) \qquad D_s \to \tau\nu \quad (26)$$

where the error is dominated by the experimental branching fraction. We can combine the results, allowing for correlated errors in f_{D_s} and τ_{D_s}, to obtain

$$V_{cs} = 1.010(22) \quad (27)$$

This central value is in a disallowed region above 1 so we also provide an alternative result that takes this into account. We divide the error above into its statistical and systematic contributions as 1.010(20)(11) and then reinterpret the statistical probability distribution as a Gaussian cutoff at 1. We then take the central value as the median of this new distribution and the error bars as encompassing $\pm$ one third of the area about the median. This procedure gives the following result:

$$V_{cs} = 0.990^{+0.007}_{-0.012} \pm 0.011. \quad (28)$$

Both these values for V_{cs} are compatible with CKM results (or V_{ud}) at better than the 2σ level. An independent direct determination of V_{cs} is possible from $D \to Kl\nu$ semileptonic decay for which it is also possible to obtain very accurate results with the HISQ action [59].

A useful bound can be obtained on the mass of a charged Higgs from comparing the experimental determination of the D_s leptonic branching fraction to the expected result using f_{D_s} from lattice QCD (i.e. standard model), see, for example, [20]. In a 2-Higgs doublet model (Type II) the D_s can also annihilate to a charged Higgs which interferes destructively with the W annihilation. This changes the leptonic branching fraction by a simple factor r, where

$$\sqrt{r} = 1 + \frac{1}{1 + m_s/m_c} \left(\frac{m_{D_s}}{m_{H^\pm}}\right)^2 \left(1 - \frac{m_s}{m_c} \tan^2\beta\right) \quad (29)$$

and $\tan\beta$ is the ratio of vacuum expectation values of the two scalar doublets. $r < 1$ for large $\tan\beta$ but this would be seen from an experimental determination of f_{D_s} (using V_{cs} from CKM unitarity) being smaller than the lattice QCD result. Thus we can derive a bound in the $\tan\beta/m_{H^\pm}$ plane from the fact that this is not the case. Here we update what was done in [20] to include our new lattice QCD result given here and the current world average f_{D_s} from experiment [25]. These combine to give a central value and error for $\sqrt{r} = 1.038(23)$, i.e. $\sqrt{r} > 0.968$ at the 3σ level. Equation (29), using our recent accurate determination of m_c/m_s from lattice QCD [36], then excludes low values of $m_{H^\pm}$ as indicated in Fig. 19. The bound is not as strong as in [20] because of the upward shift of our lattice QCD result. However the fact that our lattice result, and now the experimental average, are so accurate still means that a bound exists. New results from BES [58] with improved experimental errors would produce a much stronger bound, if the experimental central value does not change but the error on f_{D_s} is reduced to 1%. This is also indicated in Fig. 19. The exclusion limits should be compared to that from direct searches at LEP ($m_{H^\pm} > 78.6$ GeV at 95% C.L.) from [60] and the estimates of discovery potential and exclusion reach of ATLAS at LHC [61]. Reference [62] obtains a bound of $m_{H^\pm} > 316$ GeV from combining results from several processes including D/D_s leptonic decay.

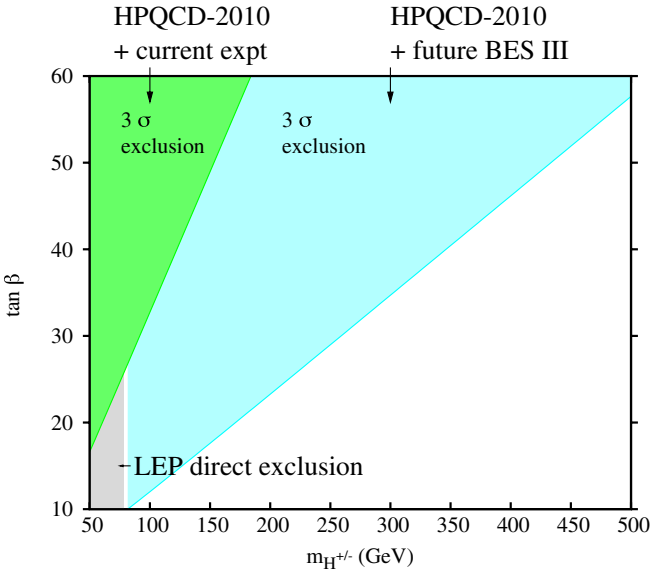

FIG. 19 (color online). Bounds in the $\tan\beta$/charged Higgs mass plane for a 2-Higgs doublet model of Type II given by our lattice QCD (i.e. standard model) result for f_{D_s} and two different experimental scenarios. The green area is excluded at 3σ by existing experimental results [25] and the light blue area will be excluded by BESIII results [58] if the central experimental value does not change. The light grey band shows the direct limit from LEP searches [60].

We have also updated results for f_π, f_K and f_D based on the change in the calibration of the lattice spacing used here for f_{D_s} but, however, with *no* new calculations in these cases. We find results consistent with experiment. Finally we have given a new very accurate result for f_{η_c} which will be useful as a calibration point for future lattice QCD calculations in charm physics.

ACKNOWLEDGMENTS

We are grateful to the MILC Collaboration for the use of their configurations. Computing was done at the Ohio Supercomputer Center and the Argonne Leadership Computing Facility at Argonne National Laboratory, supported by the Office of Science of the U.S. Department of Energy under Contract No. DOE-AC02-06CH11357.

We acknowledge the use of Chroma [66] for part of our analysis. This work was supported by the Scottish Universities Physics Alliance, STFC, MICINN, NSF and DOE.

APPENDIX: SEA-QUARK MASSES

The staggered quarks in the sea are asqtad improved staggered quarks whereas the valence quarks are HISQ quarks, i.e. they use different discretizations of the quark piece of the QCD Lagrangian. The s quark mass in the two formalisms will then not be the same, but there should be a fixed ratio between the two which is in principle calculable in perturbation theory up to discretization effects. This reflects the fact that the difference between the two Lagrangians is a difference of regularization and therefore an ultraviolet effect. Calculations in $\mathcal{O}(\alpha_s)$ perturbation theory of the mass renormalization in the two formalisms shows that the $\mathcal{O}(\alpha_s)$ term in the relative normalization is very small [28,63]. We therefore expect [64]

$$\frac{am^{\rm hisq}}{am^{\rm asq}} = 1 - 0.004\alpha_s(a) + C\alpha_s^2(a) + \ldots \qquad \text{(A1)}$$

up to discretization and sea-quark mass effects. Here $am^{\rm hisq}$ and $am^{\rm asq}$ are the lattice valence quark masses for the HISQ and asqtad actions, respectively, that give the same meson mass for a particular meson on a given ensemble. Note that $am^{\rm asq}$ is defined in the conventional way i.e. without the u_0 factor present in Table I.

Given the HISQ to asqtad mass ratio we can determine the tuning of the sea-quark masses from our tuning of the valence HISQ masses. There is very little sea-quark mass dependence in the quantities that we study here, so that we do not need to know this ratio accurately. In principle it could be done very accurately, because as we have seen the meson masses can be determined very accurately. In the absence of this information for asqtad quarks, however, we take the suggested tuned asqtad strange quark masses from the MILC Collaboration [31], correcting for the u_0 factor (taken from the lightest sea-quark mass ensemble at each lattice spacing and given in Table VI), and compare them to our tuned HISQ strange quark masses [35]. Figure 20 shows results on very coarse, coarse, fine and superfine lattices. The errors on each point are substantial, ~3%, because we have included the tuning error from each action added in quadrature, since the tunings were done in a different way. The results can easily be fit to the form:

$$\frac{am^{\rm hisq}}{am^{\rm asq}} = 1 - 0.004\alpha_s(a) + C\alpha_s^2(a) + Da^2 + Ea^4 \qquad \text{(A2)}$$

adding discretization errors to that in Eq. (A1). The fit gives a coefficient $C \approx 2$.

The fitted curve enables us to determine that the sea strange quark mass on the ultrafine lattices should be 0.0135(5) (with u_0 factor *included*) i.e. it is reasonably well-tuned. The error is substantial, but the sea-quark masses have very little impact on the accuracy of results given here.

TABLE VI. The sea asqtad masses given in Table I have a factor of u_0 equal to the fourth root of the average plaquette included in them. We remove this factor in our comparison of quark masses between HISQ and asqtad and so give values here in column 2 from [30], for all ensembles except set 7 where the result is simply estimated from that of the other coarse lattices. Column 3 gives values for the physical asqtad strange quark at each lattice spacing mass quoted by MILC [31] and including the u_0 factor. The result on set 11 is obtained from the tuned HISQ strange mass and the ratio described in the text. Columns 4 and 5 then give values for δx_l and δx_s as defined in Eq. (A3) and used in our extrapolations to the physical point. Errors come from the errors in $u_0 am_{s,\rm phys}$ and are correlated between ensembles at a given lattice spacing and between δx_l and δx_s.

Set	u_0	$u_0 am^{\rm asq}_{s,\rm phys}$	δx_l	δx_s
1	0.8604	0.0439(18)	0.184(10)	0.10(5)
2	0.8610	0.0439(18)	0.405(19)	0.10(5)
3	0.8678	0.0350(7)	0.106(3)	0.429(29)
4	0.8677	0.0350(7)	0.249(6)	0.429(29)
5	0.8677	0.0350(7)	0.249(6)	0.429(29)
6	0.8688	0.0350(7)	0.535(12)	0.429(29)
7	0.868	0.0350(7)	0.249(6)	−0.143(18)
8	0.8782	0.0261(5)	0.201(5)	0.188(23)
9	0.8788	0.0261(5)	0.439(10)	0.188(23)
10	0.8879	0.0186(4)	0.157(5)	−0.03(2)
11	0.8951	0.0135(5)	0.170(8)	0.04(4)

Table VI gives values for the u_0 parameter ($=$ (plaq)$^{1/4}$) and the physical asqtad strange quark masses given by the

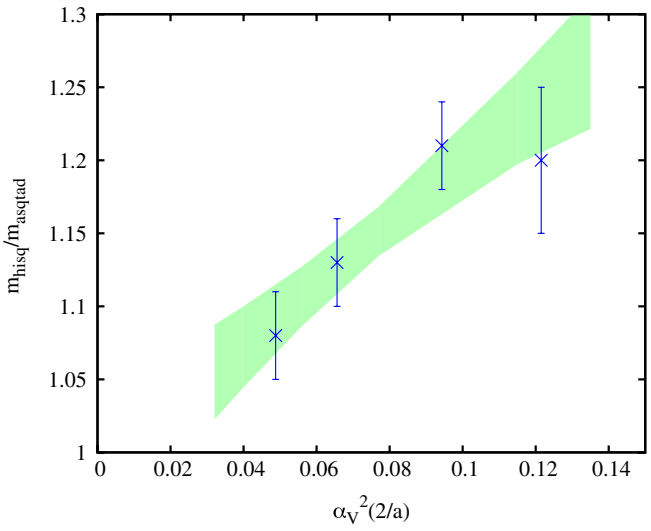

FIG. 20 (color online). Results for the ratio of the physical masses of the strange quark using the HISQ formalism [35] and the asqtad formalism [31]. The mass for the asqtad formalism in this ratio has the factor of u_0 removed. The points are lattice results combining our work and that of the MILC Collaboration. The shaded band represents a fit of the form given in Eq. (A2).

MILC Collaboration [31] for all lattice spacing values except the ultrafine. We use our result for ultrafine as discussed above. From the physical strange quark mass we determine the physical light quark mass using the MILC result: $m_s/m_l = 27.2(3)$. The table then gives values for δx_l and δx_s, where

$$\delta x_q = \frac{m_{q,\mathrm{sea}} - m_{q,\mathrm{sea,phys}}}{m_{s,\mathrm{sea,phys}}}, \tag{A3}$$

used in our extrapolation to physical quark masses in Sec. III.

[1] C. T. H. Davies *et al.* (HPQCD/Fermilab/MILC), Phys. Rev. Lett. **92**, 022001 (2004).
[2] E. B. Gregory *et al.* (HPQCD), Phys. Rev. Lett. **104**, 022001 (2010).
[3] E. Follana *et al.* (HPQCD), Phys. Rev. Lett. **100**, 062002 (2008).
[4] C. Aubin *et al.* (MILC), Phys. Rev. D **70**, 114501 (2004).
[5] G. P. Lepage, Phys. Rev. D **59**, 074502 (1999).
[6] D. Toussaint and K. Orginos (MILC), Phys. Rev. D **59**, 014501 (1998).
[7] C. Aubin *et al.* (Fermilab Lattice/MILC), Phys. Rev. Lett. **95**, 122002 (2005).
[8] A. X. El-Khadra *et al.* (Fermilab Lattice), Phys. Rev. D **55**, 3933 (1997).
[9] E. Follana *et al.* (HPQCD), Phys. Rev. D **75**, 054502 (2007).
[10] M. Artuso *et al.* (CLEO), Phys. Rev. Lett. **95**, 251801 (2005).
[11] M. Artuso *et al.* (CLEO), Phys. Rev. Lett. **99**, 071802 (2007); T. K. Pedlar *et al.* (CLEO), Phys. Rev. D **76**, 072002 (2007).
[12] B. Aubert *et al.* (*BABAR*), Phys. Rev. Lett. **98**, 141801 (2007).
[13] B. Eisenstein *et al.* (CLEO), Phys. Rev. D **78**, 052003 (2008).
[14] K. M. Ecklund *et al.* (CLEO), Phys. Rev. Lett. **100**, 161801 (2008).
[15] L. Widhalm *et al.* (BELLE), Phys. Rev. Lett. **100**, 241801 (2008).
[16] L. M. Zhang (CLEO), *Proceedings of ICHEP08* (Philadelphia, 2008), econf C080730 [arXiv:0810.2328].
[17] C. T. H. Davies (HPQCD), *Proceedings of ICHEP08* (Philadelphia, 2008), econf C080730 [arXiv:0810.3567].
[18] Proceedings of LAT2008, http://pos.sissa.it/cgi-bin/reader/conf.cgi?confid=66.
[19] B. A. Dobrescu and A. S. Kronfeld, Phys. Rev. Lett. **100**, 241802 (2008).
[20] A. G. Akeroyd and F. Mahmoudi, J. High Energy Phys. 04 (2009) 121.
[21] J. P. Alexander *et al.* (CLEO), Phys. Rev. D **79**, 052001 (2009).
[22] P. U. E. Onyisi *et al.* (CLEO), Phys. Rev. D **79**, 052002 (2009).
[23] P. Naik *et al.* (CLEO), Phys. Rev. D **80**, 112004 (2009).
[24] J. P. Lees *et al.* (*BABAR*), arXiv:1003.3063.
[25] Heavy Flavor Averaging Group, http://www.slac.stanford.edu/xorg/hfag/charm/index.html.
[26] P. del Amo Sanchez *et al.* (*BABAR*), arXiv:1008.4080.
[27] E. Follana, A. Hart, and C. T. H. Davies (HPQCD/UKQCD), Phys. Rev. Lett. **93**, 241601 (2004).
[28] E. Follana *et al.* (HPQCD/UKQCD), Phys. Rev. D **72**, 054501 (2005).
[29] See, for example, S. Sharpe, Proc. Sci., LAT2006 (2006) 022 [arXiv:hep-lat/0610094]; A. Kronfeld, Proc. Sci., LAT2007 (2007) 016 [arXiv:0711.0699].
[30] C. T. H. Davies *et al.* (HPQCD), Phys. Rev. D **78**, 114507 (2008).
[31] A. Bazavov *et al.*, Rev. Mod. Phys. **82**, 1349 (2010).
[32] C. T. H. Davies *et al.*, Proc. Sci., LAT2008 (2008) 118 [arXiv:0810.3548].
[33] S. Naik, Nucl. Phys. **B316**, 238 (1989).
[34] P. Lepage *et al.*, Nucl. Phys. B, Proc. Suppl. **106**, 12 (2002).
[35] C. T. H. Davies *et al.* (HPQCD), Phys. Rev. D **81**, 034506 (2010).
[36] C. T. H. Davies *et al.* (HPQCD), Phys. Rev. Lett. **104**, 132003 (2010).
[37] Particle Data Group, http://pdg.lbl.gov/.
[38] E. Gregory *et al.* (HPQCD), arXiv:1010.3848.
[39] J. L. Goity and C. P. Jayalath, Phys. Lett. B **650**, 22 (2007).
[40] A. Bazavov *et al.* (MILC), Phys. Rev. D **82**, 074501 (2010).
[41] See, for example, L. H. Ryder, *Quantum Field Theory* (Cambridge University Press, Cambridge, England, 1985).
[42] E. Gamiz *et al.* (HPQCD), Phys. Rev. D **80**, 014503 (2009); C. Bernard *et al.* (Fermilab Lattice/MILC), Proc. Sci., LAT2008 (2008) 278 [arXiv:0904.1895]; B. Blossier *et al.* (ETMC), Proc. Sci., LAT2009 (2009) 151 [arXiv:0911.3757].
[43] Note that experimental results also include electromagnetic radiation effects that are specifically excluded from the definition of f_{D_s} and must be subtracted before a value is derived from experiment. See the review by J. Rosner and S. Stone in [37].
[44] T. Burch *et al.*, (Fermilab Lattice/MILC), Phys. Rev. D **81**, 034508 (2010).
[45] C. Bernard *et al.* (Fermiab Lattice/MILC), arXiv:1003.1937.
[46] A. Bazavov *et al.*, Proc. Sci., LAT2009 (2009) 249 [arXiv:0912.5221].
[47] A. X. El-Khadra *et al.*, Proc. Sci., LAT2007 (2007) 242 [arXiv:0710.1437].
[48] In fact clover quarks (which is what Fermilab quarks become in the light quark mass limit) have some difficulties in reproducing values for f_π and f_K with the renormalization procedures being currently used. See C.

McNeile, Proc. Sci., LAT2007 (2007) 019 [arXiv:0710.0985]; K. Jansen, Proc. Sci., LAT2008 (2008) 010 [arXiv:0810.5634].
[49] B. Blossier *et al.* (ETMC) J. High Energy Phys. 07 (2009) 043.
[50] R. Baron *et al.* (ETMC), J. High Energy Phys. 06 (2010) 111.
[51] A. S. Kronfeld, arXiv:0912.0543.
[52] P. Dimopoulos *et al.* (ETMC), Proc. Sci., LAT2008 (2008) 106 [arXiv:0810.1220].
[53] A. O. Cais *et al.*, arXiv:0801.0973.
[54] C. Ehmann and G. Bali, Proc. Sci., LAT2007 (2007) 094 [arXiv:0710.0256].
[55] W. Kwong and J. L. Rosner, Annu. Rev. Nucl. Part. Sci. **37**, 325 (1987).
[56] K. W. Edwards *et al.* (CLEO), Phys. Rev. Lett. **86**, 30 (2001).
[57] J. Erler, Phys. Rev. D**59**, 054008 (1999).
[58] D. Asner *et al.*, arXiv:0809.1869.
[59] H. Na *et al.*, (HPQCD), arXiv:1008.4562.
[60] LEP Higgs Working Group, note submitted to Lepton-Photon01, arXiv:hep-ex/0107031.
[61] M. Flechl (ATLAS Collaboration), Proc. Sci., CHARGED2008 (2008) 006.
[62] O. Deschamps *et al.* (CKMfitter), arXiv:0907.5135.
[63] Q. Mason *et al.* (HPQCD), Phys. Rev. D **73**, 114501 (2006).
[64] In [35] we used a different, more phenomenological, form for the HISQ to asqtad mass ratio using results from matching meson masses on coarse and fine lattices.
[65] Note that the Heavy Flavor Averaging Group adjusts the result from [12] to account for the fact that it was normalized to $D_s \to \phi\pi$ and this latter branching fraction has to be corrected for the mass window applied for ϕ reconstruction.
[66] R. G. Edwards and B. Joo, Nucl. Phys. B, Proc. Suppl. **140**, 832 (2005).